

TLR4-induced NF- κ B and MAPK signaling regulate the IL-6 mRNA stabilizing protein Arid5a

Kishan K. Nyati¹, Kazuya Masuda¹, Mohammad Mahabub-Uz Zaman¹, Praveen K. Dubey¹, David Millrine¹, Jaya P. Chalise¹, Mitsuru Higa¹, Songling Li², Daron M. Standley², Kazunobu Saito³, Hamza Hanieh⁴ and Tadimitsu Kishimoto^{1,*}

¹Laboratory of Immune Regulation, World Premier International Immunology Frontier Research Center, Osaka University, Osaka 565-0871, Japan, ²Laboratory of System Immunology, World Premier International Immunology Frontier Research Center, Osaka University, Osaka 565-0871, Japan, ³Central Instrumentation Laboratory, Research Institute of Microbial Diseases, Osaka University, Osaka 565-0871, Japan and ⁴Biological Sciences Department, College of Science, King Faisal University, Al-Ahsa 31982, Saudi Arabia

Received September 10, 2016; Revised January 23, 2017; Editorial Decision January 24, 2017; Accepted February 06, 2017

ABSTRACT

The AT-rich interactive domain-containing protein 5a (Arid5a) plays a critical role in autoimmunity by regulating the half-life of Interleukin-6 (IL-6) mRNA. However, the signaling pathways underlying Arid5a-mediated regulation of IL-6 mRNA stability are largely uncharacterized. Here, we found that during the early phase of lipopolysaccharide (LPS) stimulation, NF- κ B and an NF- κ B-triggered IL-6-positive feedback loop activate *Arid5a* gene expression, increasing IL-6 expression via stabilization of the IL-6 mRNA. Subsequently, mitogen-activated protein kinase (MAPK) phosphatase-1 (MKP-1) promotes translocation of AU-rich element RNA-binding protein 1 (AUF-1) from the nucleus to the cytoplasm, where it destabilizes *Arid5a* mRNA by binding to AU-rich elements in the 3' UTR. This results in downregulation of IL-6 mRNA expression. During the late phase of LPS stimulation, p38 MAPK phosphorylates Arid5a and recruits the WW domain containing E3 ubiquitin protein ligase 1 (WWP1) to its complex, which in turn ubiquitinates Arid5a in a K48-linked manner, leading to its degradation. Inhibition of Arid5a phosphorylation and degradation increases production of IL-6 mRNA. Thus, our data demonstrate that LPS-induced NF- κ B and MAPK signaling are required to control the regulation of the IL-6 mRNA stabilizing molecule Arid5a. This study therefore substantially increases our understanding of the mechanisms by which IL-6 is regulated.

INTRODUCTION

The innate immune responses that are triggered by the classic inflammatory stimulus lipopolysaccharide (LPS) are mediated by toll-like receptor (TLR) 4 and subsequent activation of the transcription factors NF- κ B and AP-1 (1). These transcription factors are, in turn, responsible for the transcriptional activation of a set of genes that mediate inflammation, among which interleukin-6 (IL-6) is particularly important (1,2). Abnormal expression of IL-6 has been associated with the pathogenesis of a variety of human diseases, including cancers and autoimmune and inflammatory diseases (3). Therefore, it is critical that cells control the expression of IL-6, from synthesis to degradation.

The expression of IL-6 is tightly regulated at multiple levels, including gene transcription, mRNA translation and mRNA degradation levels (4,5). Transcriptional regulation of gene expression is essential; however, transcription cannot be rapidly inhibited or redirected. Multiple biological networks tightly control this regulatory mechanism. Post-transcriptional regulatory mechanisms, including those that function via RNA-binding proteins (RBPs), are required to modulate mRNA levels and thus can rapidly affect protein expression. Regnase-1 has been shown to destabilize IL-6 mRNA by interacting with a conserved stem-loop motif in the 3' untranslated region (UTR) that is distinct from AU-rich elements (AREs) (6). Recently, we showed that AT-rich interactive domain-containing protein 5A (Arid5a) competes with Regnase-1 to regulate IL-6 (7). Arid5a post-transcriptionally regulates IL-6 by binding to the 3' UTR of the IL-6 mRNA at the same site at which Regnase-1 attaches, interfering with Regnase-1-mediated destabilization of IL-6 and contributing to the production of IL-6 expression *in vivo* (7). The I κ B kinase (IKK) complex has been

*To whom correspondence should be addressed. Tel: +81 668 794 957; Fax: +81 668 794 958; Email: kishimoto@ifrec.osaka-u.ac.jp
Present address: Praveen Kumar Dubey, Department of Anesthesiology and Perioperative Medicine, School of Medicine, University of Alabama, Birmingham, AL 35294, USA

shown to control IL-6 mRNA stability by phosphorylating Regnase-1 in response to stimulation by the TLR or IL-1 receptor (8). However, the signaling pathways that mediate the stabilization of IL-6 by Arid5a remain unknown.

The mitogen-activated protein kinase (MAPK) signaling pathway, which includes p38 MAPK and MAPK phosphatase-1 (MKP-1) signaling, plays an important role in regulating the functions of RBPs and the expression levels of inflammatory cytokines (9–13). The initial activation of p38 MAPK was found to be responsible for the expression of the early-response gene MKP-1 (14). Once activated, the phosphatase activity of MKP-1 increases the degradation of cytokine mRNAs by dephosphorylating p38 MAPK. However, during the late phase, MKP-1 is down-regulated and p38 MAPK engages in other immune functions (15). P38 MAPK phosphorylates an RBP named tristetraprolin (TTP) and facilitates the degradation of TNF- α mRNA (16). P38 MAPK signaling has also been shown to stabilize the mRNA of the cell cycle regulatory protein p21^{Cip1} by phosphorylating the RBP HuR (17). Thus, p38 MAPK is involved in regulating a variety of signaling pathways, including those involved in the stability of mRNA critical for both innate and acquired immunity (18).

Although Arid5a mRNA expression is induced in response to TLR4 stimulation, the regulation of Arid5a protein during stabilization of IL-6 mRNA has not been fully explored. In the present study, we found that IKK signaling transcriptionally activates Arid5a gene expression in macrophages in response to stimulation by TLR4. This was followed by the activation of MKP-1, which led to the destabilization of Arid5a mRNA by RBP AU-rich element RNA-binding protein 1 (AUF-1). During the late phase of LPS stimulation, Arid5a is phosphorylated by p38 MAPK, leading to its degradation via K48-linked ubiquitination by the WW domain containing E3 ubiquitin protein ligase 1 (WWP1). Our data showed that regulation of Arid5a by NF- κ B and MAPK signaling is required to maintain the balance of IL-6 mRNA expression.

MATERIALS AND METHODS

Mice and reagents

C57BL/6 wild-type (WT) mice (6–8 weeks old) were obtained from CLEA, Japan. Mice were maintained under specific pathogen-free conditions. All animal experiments were performed in accordance with protocols approved by the Institutional Animal Care and Use Committee of Osaka University. LPS (*Escherichia coli*: 055:B5), Actinomycin D, U0126 (MEK1/2 inhibitor), SP600125 (JNK inhibitor), BMS345541 (I kappa B kinase inhibitor), LY249005 (PI3K inhibitor) and phosphatase inhibitor cocktail 2 and 3 were obtained from Sigma-Aldrich. Recombinant murine IL-6 was obtained from Peprotech, MG-132 (proteasome inhibitor) was obtained from Calbiochem, SB203580 (p38 MAP kinase inhibitor) was obtained from Abcam and Stat3 Inhibitor VI (S3I-201) was obtained from Santa Cruz Biotechnology.

Cell culture and transfection

Thioglycollate-stimulated peritoneal macrophages were cultured in Roswell Park Memorial Institute (RPMI) medium 1640 (Sigma-Aldrich) containing 10% (vol/vol) foetal bovine serum (FBS), 100 μ g/ml streptomycin, 100 U/ml penicillin G (Nacalai Tesque) and 50 μ M β -mercaptoethanol. Primary mouse embryonic fibroblasts (MEFs) were prepared from WT mouse and Arid5a-deficient embryos at embryonic day 13.5. HEK293TLR4/MD2/CD14 cells were purchased from InvivoGen. IKK β ^{-/-} MEFs were kindly provided by Dr Hiroki Tanaka. MEFs and HEK293TLR4/MD2/CD14 cells were maintained in Dulbecco's modified Eagle's medium (DMEM) (Nacalai Tesque) supplemented with 10% (vol/vol) FBS, 100 μ g/ml streptomycin and 100 U/ml penicillin G (Nacalai Tesque). Cells were transfected using Lipofectamine LTX (Invitrogen).

Plasmid construction

The Myc and Flag-tagged Arid5a expression vectors have been previously described (19). The expression plasmids containing K48-HA-Ub, p65 and c-Rel were purchased from Addgene, and the expression plasmid containing p38 (RDB08163) was purchased from Riken Biological Resources, Japan. The expression plasmid containing hemagglutinin-tagged ubiquitin and Flag-STAT3 were kindly provided by Prof. Masahiro Yamamoto, the plasmid containing pCMV-AUF-1 was a gift from Prof. S. Akira and Dr T. Satoh, and the Flag-JNK-1 and Flag-JNK-2 plasmids were obtained from Prof. Katsuji Yoshioka. The expression vectors v5-IKK α , v5-IKK β , v5-IKK ϵ and v5-IRAK1 were prepared in our laboratory using a pcDNA3.1 v5-his TOPO TA expression kit (Thermo Fisher Scientific) according to the manufacturer's instructions. WWP1 cDNA was cloned into the vector pcDNA3.1(+)-Flag at EcoRI and XbaI restriction sites to induce its expression using an In-fusion HD cloning kit (Clontech). Point mutations were made in the gene encoding Arid5a (substitutions S253A, S433A, S458A, K80R and K89R), STAT3 (substitutions Y705F and S727A) and p65 (substitutions S536A and K310R/K314R/K315R) using a KOD-Plus-Mutagenesis Kit (Toyobo). The cDNA was ligated to the vector pcDNA3.1(+)-Flag to induce its expression. The 3' UTR of the mouse Arid5a mRNA and the promoter of the mouse Arid5a gene were amplified using polymerase chain reaction (PCR) from mouse genomic DNA and then ligated into the pGL3 vector (Promega).

Immunoblot analysis

Whole-cell extracts were prepared in Radioimmunoprecipitation assay (RIPA) lysis buffer or IP lysis buffer (Pierce) supplemented with Complete Protease Inhibitor Cocktail (Nacalai Tesque). Nuclear and cytoplasmic proteins were extracted using NE-PER nuclear and cytoplasmic extraction reagents (Thermo Fisher Scientific) according to the manufacturer's instructions. The following antibodies were used for the immunoblot assays: anti-Arid5a (ab81149; Abcam), anti-AUF-1, (07-260; Millipore), anti-MKP-1 (373841; Santa Cruz), anti-c-Rel (sc-6955x; Santa

Cruz), anti-p65 (sc-372x; Santa Cruz), anti-p52 (4882; Cell Signaling Technology), anti-STAT3 (9139; Cell Signaling Technology), anti-p38 (9212; Cell Signaling Technology), anti-Lamin A/C (2032; Cell Signaling Technology), anti- β -tubulin (2146; Cell Signaling Technology), anti- β -actin (4970; Cell Signaling Technology), anti-GAPDH (5174; Cell Signaling Technology), anti-phosphoserine (ab6639; Abcam), anti-Myc (2276; Cell Signaling Technology), anti-Myc-HRP (M047-7; MBL), anti-hemagglutinin (3724; Cell Signaling Technology), anti-hemagglutinin-HRP (M180-7; MBL), anti-Flag M2 (A8592; Sigma), anti-Flag M2 gel (A2220; Sigma) and anti-v5-HRP (46-0708; Invitrogen). The control mouse (sc2025) and rabbit (sc2027) IgGs were purchased from Santa Cruz Biotechnology. Luminescence was detected using a luminescent image analyzer (ImageQuant LAS 4000).

RNA binding assay

RNA binding assays were performed according to the protocol included with the RiboTrap Kit (MBL International). Briefly, 5-bromo-UTP (BrU) was randomly incorporated into the 3' UTR of the Arid5a mRNA upon its transcription using a pBluescript plasmid containing the Arid5a 3' UTR. Anti-BrdU antibodies were conjugated to protein G beads. Then, the Arid5a 3' UTR was bound to the beads. Peritoneal macrophages were stimulated using LPS or were not stimulated (controls). Then, the cell lysates from each experiment were transferred to antibody-conjugated beads with the BrU-labeled Arid5a 3' UTR for 2 h. The samples were washed and eluted, and they were then subjected to sodium dodecyl sulphate-polyacrylamide gel electrophoresis (SDS-PAGE).

Luciferase assay

HEK293 cells or MEF cells were transfected with pGL3-luciferase plasmids encoding the Arid5a 3' UTR, the Arid5a promoter or pGL3-luciferase plasmid (control). All transfections were performed in combination with one of the following: WT AUF-1, c-Rel, p65, mutant p65 (S536A and K310R/K314R/K315R) and STAT3 and mutant STAT3 (Y705F and S727A) expression plasmids, or an empty (control) plasmid. At 24–48 h after transfection, the cells were lysed. The luciferase activity in the lysates obtained from treated samples was determined using a Dual Luciferase Reporter Assay System (Promega). The *Renilla* luciferase gene was simultaneously transfected as an internal control.

Chromatin immunoprecipitation (ChIP) assay

NF- κ B (p65, c-Rel) and STAT3 binding to the Arid5a promoter region was quantified in mouse peritoneal macrophages using ChIP-qPCR. The ChIP analyses were performed using a ChIP assay kit (Upstate) according to the manufacturer's instructions. Briefly, peritoneal macrophages were cultured and stimulated using LPS (1–10 μ g/ml). Chromatin (5 μ g) was prepared and then immunoprecipitated using ChIP-grade antibodies against p65, c-Rel and STAT3 (4 μ g each). Normal IgG (4 μ g) was used

as a control. The number of DNA fragments that was precipitated using Protein-G Dynabeads (Novex) was quantified using the SYBR Green (Roche) method in combination with real-time qPCR using Arid5a-specific primer pairs. The sequences of these primers are listed in Supplementary Table S1.

Quantitative PCR analysis

A RNeasy Mini Kit (Qiagen) was used to isolate RNA. cDNA was prepared using a QuantiTect Reverse Transcription Kit (Qiagen) according to the manufacturer's instructions. RT-PCR was performed using an ABI PRISM 7900 HT (Applied Biosystems) with FastStart Universal SYBR Green master mix (Life Technologies), and the results were normalized to the level of GAPDH mRNA. The primers used to amplify each PCR product are shown in Supplementary Table S2. Values are expressed as a fold induction compared to that of the unstimulated control condition.

Knockdown assay

Mouse IL-6, AUF-1, MKP-1, p65, p52, STAT3, WWP1, Artogin1, Trim29, Trim38 and Smurf1 siRNAs and the scramble siRNA (control) were purchased from Invitrogen. MEF cells were transfected with siRNAs (10–20 nM each) or scramble siRNA (control) for 72 h. Transfections were performed using RNAiMAX (Thermo Fisher Scientific) reagents according to the protocol provided by the manufacturer.

Stability of mRNA

Actinomycin D (2, 3 or 5 μ g/ml; Sigma) was added directly to cell cultures that were previously treated with or without LPS. Cells were incubated for the appropriate amount of time after the addition of Actinomycin D. The results were analyzed using real-time qPCR analysis to determine the mRNA levels, as described above.

RNA EMSA

Electrophoretic mobility shift assay (EMSA) was performed according to the protocol provided with the Light-Shift Chemiluminescent RNA EMSA kit (Thermo Fisher Scientific), which has been previously described (20). The RNA was synthesized as single strand and then 3'-end labeled with biotin (Hokkaido System Science). The following sequences were used: 5'-AGUCACAGUGAUU UUACCUGGUUGCUC-3' and 5'-GAUGACUUAG GCUGCAUUUAGAACCUUCA-3'. The recombinant AUF-1 protein was purchased from Abcam.

Immunoprecipitation

HEK293TLR4, or MEF cells were seeded in 60 or 100 mm dishes and transiently transfected with a total of 4–5 μ g of the appropriate combination of plasmids. At 24–48 h after transfection, the cells were lysed in lysis buffer (described above). Proteins were immunoprecipitated from the lysates overnight using the appropriate antibodies and

protein G Sepharose 4 Fast Flow (GE Healthcare) in lysis buffer. The collected immune complexes were washed four times with lysis buffer and then suspended in SDS sample buffer (Nacalai Tesque). The samples were boiled for 5 min at 96°C and then separated using SDS-PAGE.

Ubiquitination assay

These assays were performed using a previously described protocol, with some modifications (8). Transfected HEK293TLR4 cells or MEFs cells were incubated for 6–9 h with MG-132 (1 μM) before they were collected. The cell lysates were sonicated in 1% (wt/vol) SDS to remove any non-covalently attached proteins and then immunoprecipitated using anti-Flag/anti-Myc and protein G Sepharose 4 Fast Flow in 0.1% (wt/vol) SDS lysis buffer in the presence of protease inhibitors and MG-132 (1 μM). Ubiquitin was detected using immunoblot assays.

Enzyme-linked immunosorbent assay (ELISA)

Enzyme-linked immunosorbent assay was used to measure the levels of mouse IL-6 in the supernatants obtained from WT and knockdown MEF cell cultures according to the manufacturer's instructions (R&D Systems).

Protein–RNA docking

First, a structural model of the AUF-1 protein (residues 95–259) was built by homology modeling using PDB entry 1g2e chain A as a template (sequence identity: 22%). The structure of the RNA fragment AUUUA was taken from the same PDB entry 1g2e chain B, which is in contact with the template chain A. The RNA chain has two tandem AUUUA fragments (sequence: UAUUUAUUUA). The fragment close to the 3' terminal, which has more contacts with the protein, was selected. The AUF-1 homology model was first superimposed onto the template chain; then, the superimposed RNA structure was extracted. Flexible RNA docking was then carried out using coarse-grained molecular dynamics simulations with the ESPResSo (21) package and protein–RNA binding propensities (22). Amino acids were represented by a single-bead model that was fixed during the simulation. The AUUUA RNA strand was represented by five beads, and a soft core potential was introduced between the protein and the RNA so that the RNA could not enter the core region of the protein. The aaRNA binding potential of each amino acid was used as an additional contact potential to sample reliable RNA-binding conformations (22). The simulation was initialized with 100 RNA molecules randomly distributed around the protein. A total of 10,000 snapshots were stored and grouped by dynamic clustering with a threshold of 1 Å, resulting in 872 clusters. For each cluster representative, the local density was estimated as the number of total beads from all other representative models within 1.0 Å. Finally, models with a local density lower than the 0.8 quantile of all densities were removed.

Statistical analysis

All data are expressed as the mean ± SD. The results were analyzed using Student's *t*-test, and *P*-values < 0.05 were

considered statistically significant (**P* < 0.05, ***P* < 0.01 and ****P* < 0.001).

RESULTS

NF-κB upregulates *Arid5a* gene expression in response to TLR4 activation

Our group previously demonstrated that *Arid5a* mRNA is rapidly induced and degraded in macrophages following TLR4 activation (7). Therefore, we sought to identify the underlying signaling pathways. To determine how *Arid5a* expression is regulated, we first analyzed the mRNA and protein levels of *Arid5a* following stimulation with TLR4. Peritoneal macrophages were stimulated with LPS for various durations (0–24 h) *in vitro*. Both *Arid5a* mRNA expression (Figure 1A) and protein (Figure 1B) levels were observed to steadily increase during the first 4 h of stimulation. They, then gradually decreased over the next 24 h. We next investigated the mechanisms underlying the observed upregulation and subsequent decay of *Arid5a*.

When TLR4 is activated by its ligand, it activates IKK and p38 MAPK signaling (1,2,13), which are critical for robust LPS-induced production of cytokines. To investigate the potential of p38 MAPK or IKK to mediate signaling resulting in *Arid5a* gene expression, we used the pharmacological inhibitors U0126, LY294002, SP600125, SB203580 and BMS-345541, which selectively inhibit MEK1/2, PI3K, JNK, p38 and IKK, respectively. Among these signaling inhibitors, only BMS-345541, which blocks IKK (Figure 1C), showed a strong inhibitory effect on *Arid5a* gene expression. We further found that *Arid5a* gene expression was significantly reduced in IKKβ-deficient MEF cells compared to that of WT cells following LPS stimulation (Figure 1D), suggesting that IKK signaling may be a key regulator of *Arid5a* gene expression. Because IKK signaling further activates NF-κB, we next investigated the role of NF-κB in *Arid5a* expression. To confirm the role of NF-κB in mediating *Arid5a* gene expression, we transfected NF-κB (p65/c-Rel) expression constructs in combination with an *Arid5a* promoter-driven luciferase reporter into HEK293 cells. Overexpressing NF-κB (p65/c-Rel) augmented *Arid5a* promoter activity, suggesting that NF-κB is essential for the expression of *Arid5a* (Figure 1E). The nuclear functions of NF-κB p65 are known to be regulated in part by post-translational modifications of its RelA subunit, including phosphorylation and acetylation. Moreover, the phosphorylated and acetylated forms of p65 exhibit enhanced transcriptional activity (23). Therefore, to determine the binding site(s) of p65 protein that promotes transcriptional activity of the *Arid5a* gene, we mutated WT p65 at the phosphorylation and acetylation sites (S536A and K310R/K314R/K315R) and measured the luciferase activity of the *Arid5a* promoter following their transfection into HEK293 cells. Overexpressing the p65 mutant (K310R/K314R/K315R) failed to increase the *Arid5a* promoter activity compared to that of the WT and the phosphorylation mutant of p65, suggesting that the acetylation sites on p65 are important for transcriptional activation of the *Arid5a* promoter (Figure 1F).

Having confirmed that overexpressing NF-κB enhances *Arid5a* promoter activity, we next examined the binding

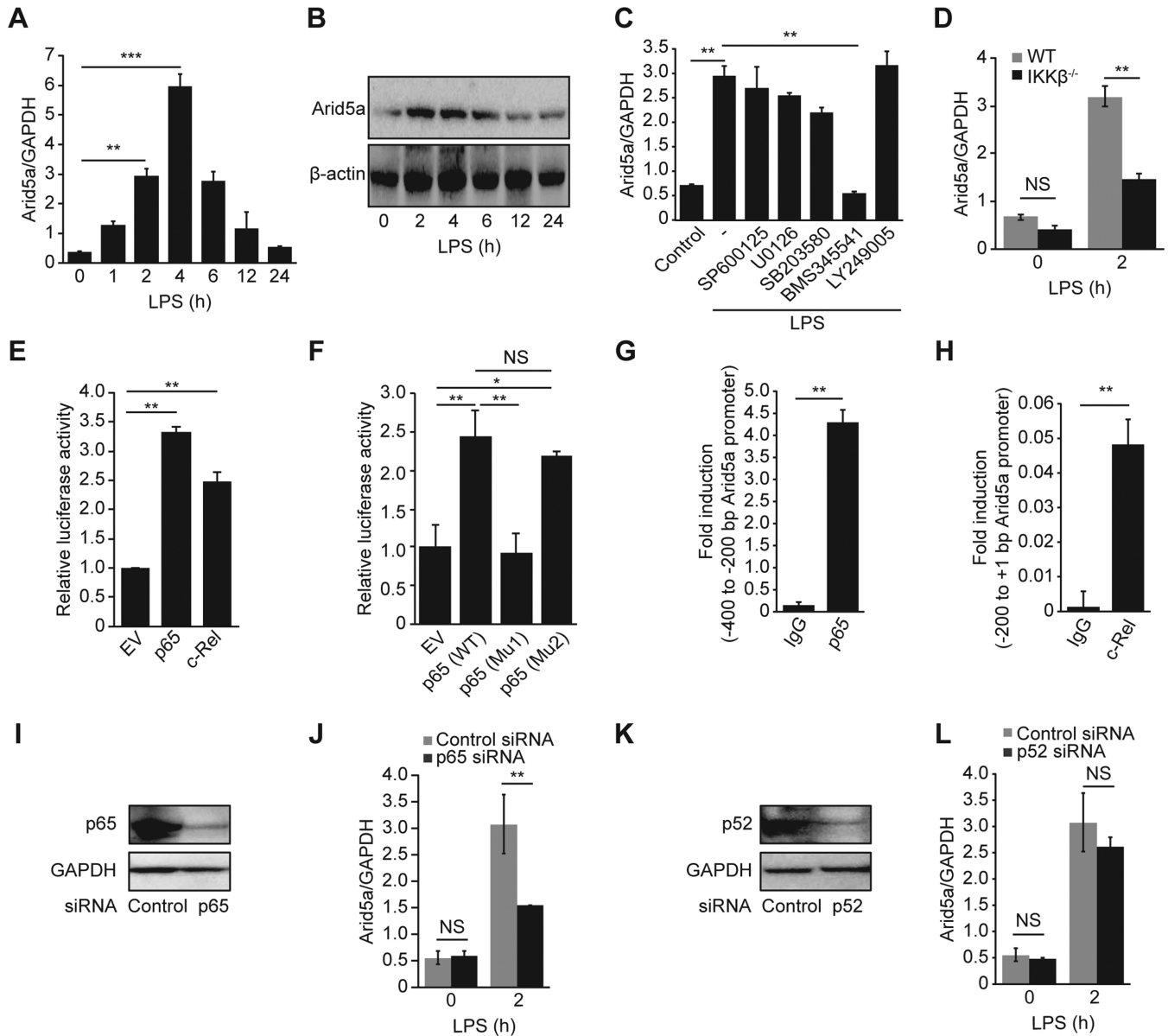


Figure 1. NF-κB induces the expression of Arid5a by binding to its promoter in response to lipopolysaccharide (LPS). (A and B) Expression of Arid5a mRNA and protein in mouse peritoneal macrophages stimulated for 0–24 h with LPS (1 μg/ml). (C) Expression of Arid5a mRNA in macrophages that were pretreated with the indicated inhibitors (10 μM) or DMSO (control) for 30 min and then stimulated with LPS for 2 h. (D) Arid5a mRNA expression in the control and IKKβ-deficient MEFs after stimulation with LPS (10 μg/ml). (E and F) HEK293T cells were transfected with a pGL3-luciferase vector encoding an Arid5a promoter (–2000 bp upstream of the TSS) or a pGL3 empty vector. Both were transfected with an empty vector (control) or with expression vectors of p65 or c-Rel (E) or p65 mutants (Mu1 and Mu2) (F). p65 Mu1 and p65 Mu2 refer to the K310R/K314R/K315R and S536A mutants, respectively. Luciferase activity was determined 24 h after transfection and normalized to the activity induced by the pGL3-empty vector. The values are shown relative to those after transfection with the empty vector. (G and H) Peritoneal macrophages were stimulated using LPS for 2 h, and ChIP assays were then performed using anti-p65, anti-c-Rel, and anti-IgG (negative control) antibodies. (I) Immunoblot assays of p65 expression in MEF cells transfected with 20 nM control or p65 siRNA. (J) Arid5a mRNA expression in the control and p65 knockdown MEFs after stimulation with LPS (10 μg/ml). (K) Immunoblot assays of p52 expression in MEF cells transfected with 20 nM control or p52 siRNA. (L) Arid5a mRNA expression in the control and p52 knockdown MEFs after stimulation with LPS (10 μg/ml). All data show the mean ± SD of three independent experiments. Error bars indicate the mean ± SD. NS, not significant; **P* < 0.05; ***P* < 0.01; ****P* < 0.001.

affinity of NF- κ B (p65/c-Rel) to *Arid5a* promoter regions using ChIP assays. After stimulation with LPS, intact peritoneal macrophage cells were fixed in formaldehyde. The cells were then lysed, and their chromatin was isolated. The isolated chromatin was then sonicated, and chromatin fragments containing proteins of interest and associated *Arid5a* DNA were selectively precipitated using ChIP-grade p65- and c-Rel-specific antibodies. Then, specific *Arid5a* DNA sequences were examined via qPCR using primers specific for the *Arid5a* promoter (−200 to −400 bp and −200 to +1 bp upstream of the TSS; Supplementary Table S1). Data from these ChIP assays revealed that the transcription factor NF- κ B-p65 bound at −400 to −200 bp (Figure 1G), while the transcription factor NF- κ B-c-Rel bound at −200 to +1 bp (Figure 1H) of the *Arid5a* promoter region. Since p65 has a transactivation domain but p52 does not, we generated p65 and p52 knockdown MEFs using p65 and p52-specific siRNAs and assessed *Arid5a* mRNA expression after LPS treatment. We found significantly lower expression in the p65 knockdown MEFs, but not in the p52 knockdown MEFs, than that in their control counterparts (Figure 1I–L). Taken together, these data suggest that NF- κ B (p65 and c-Rel) binds tightly to the promoter region of *Arid5a*, resulting in its transcriptional upregulation.

IL-6-STAT3 signaling induces *Arid5a* gene expression in response to LPS

We previously reported that *Arid5a* mRNA is upregulated following IL-6 stimulation in macrophages and MEF cells (7). Therefore, it is likely that an IL-6-positive feedback loop that responds to TLR4 signaling regulates *Arid5a* expression. To confirm this hypothesis, we first determined the expression of *Arid5a* mRNA following IL-6 stimulation in MEF cells. As expected, *Arid5a* expression was significantly upregulated within 1 h of stimulation by IL-6 (Figure 2A).

To determine whether *Arid5a* is regulated via a TLR4-mediated IL-6-positive feedback loop, we generated IL-6 knockdown MEF cells using IL-6-specific siRNA (Figure 2B). We then evaluated the expression of *Arid5a* mRNA compared to that of the controls and LPS-stimulated cells. Our data showed that knockdown of IL-6 decreased *Arid5a* mRNA expression (Figure 2C), suggesting that LPS-induced IL-6 also regulates *Arid5a* mRNA expression.

The IL-6 signaling pathway is induced by the IL-6 receptor and mediated by STAT3 activation. We therefore further investigated the role of STAT3 in regulating *Arid5a* expression. For these experiments, MEF cells were pre-treated with a pharmacological inhibitor of STAT3 (S3I-201) and then stimulated with IL-6. S3I-201 strongly inhibited *Arid5a* gene expression (Figure 2D). Similar results were found in STAT3-specific knockdown MEFs upon IL-6 stimulation (Figure 2E and F), suggesting that IL-6-STAT3 signaling induces *Arid5a* expression. To confirm the involvement of IL-6-STAT3 signaling in the *Arid5a* gene expression under TLR4 signaling, we assessed *Arid5a* mRNA expression in S3I-201-inhibited STAT3 MEFs following stimulation with LPS. We found significantly lower *Arid5a* mRNA expression in STAT3-inhibited MEFs compared to that of its counterparts (Figure 2G), suggesting that an IL-6 positive feedback loop augmented *Arid5a* expression via

activation of STAT3 in response to TLR4 signaling. As with p65, we detected the STAT3 binding region/site in the *Arid5a* promoter, mutated WT STAT3 at its two phosphorylation sites (Y705F and S536A) and measured luciferase activity of the *Arid5a* promoter after 36 h of transfection into HEK293 cells. We observed that overexpressing both STAT3 phosphorylation mutants failed to increase the *Arid5a* promoter activity compared to that of the WT, suggesting that phosphorylated STAT3 binds to the promoter region of *Arid5a* and activates its gene expression (Figure 2H). Moreover, overexpressing STAT3 significantly increased *Arid5a* promoter activity, suggesting that STAT3 is required for the expression of *Arid5a* (Figure 2H). We next examined the binding affinity of STAT3 to the *Arid5a* promoter region using ChIP assay in peritoneal macrophages following LPS stimulation as described above in Figure 1. Data from ChIP assay showed that the transcription factor STAT3 bound at −888 to −1098 (Figure 2I) of the *Arid5a* promoter region. Taken together, these data suggest that an IL-6 positive feedback loop upregulates *Arid5a* expression via STAT3 in response to TLR4 stimulation (Figure 2J).

AUF-1 binds to the 3' UTR of the *Arid5a* mRNA, resulting in its destabilization

Our data indicated that *Arid5a* expression is upregulated by an NF- κ B-mediated mechanism during the early phase of TLR4 activation. However, *Arid5a* mRNA is gradually downregulated following treatment with LPS (Figure 1A). To determine how *Arid5a* mRNA is degraded, we next focused on the post-transcriptional mechanisms that regulate *Arid5a*. To determine whether RBPs regulate *Arid5a* mRNA stability, we performed RiboTrap RNA–protein binding assays. Because *cis*-acting elements in the 3' UTR of mRNA have been shown to be required to regulate mRNA stability (24), RiboTrap was performed using the 3' UTR region of *Arid5a*. Peritoneal macrophages were stimulated with or without LPS (1 μ g/ml). The whole-cell lysates were then mixed with *Arid5a* 3' UTR (containing BrdU)-conjugated protein G beads, and the mixture was then washed. The eluted materials were subjected to SDS-PAGE analysis. Candidate bands were detected using Coomassie brilliant blue (CBB) staining and analyzed using LC-MS/MS. The profiling data of all bands between 35 and 50 kDa revealed that AUF-1 was capable of binding to the *Arid5a* 3' UTR following stimulation with LPS (Figure 3A).

To confirm the validity of this observation, we generated AUF-1 knockdown MEFs using AUF-1 specific siRNA (Figure 3B and C). *Arid5a* mRNA and protein expression and IL-6 mRNA expression were assessed in WT and AUF-1 knockdown MEFs that were treated with LPS and found to be significantly higher in the AUF-1 knockdown MEFs than that in their control counterparts. These data support the hypothesis that AUF-1 is involved in regulating the stability of *Arid5a* mRNA (Figure 3D–F).

AUF-1 has previously been shown to bind with high affinity to selected AREs and to have a destabilizing effect on ARE-mRNAs (25). To further validate these findings, we transfected MEFs with a pGL3-luciferase vector that encoded the *Arid5a* 3' UTR (3.5 kb) or fragments that ei-

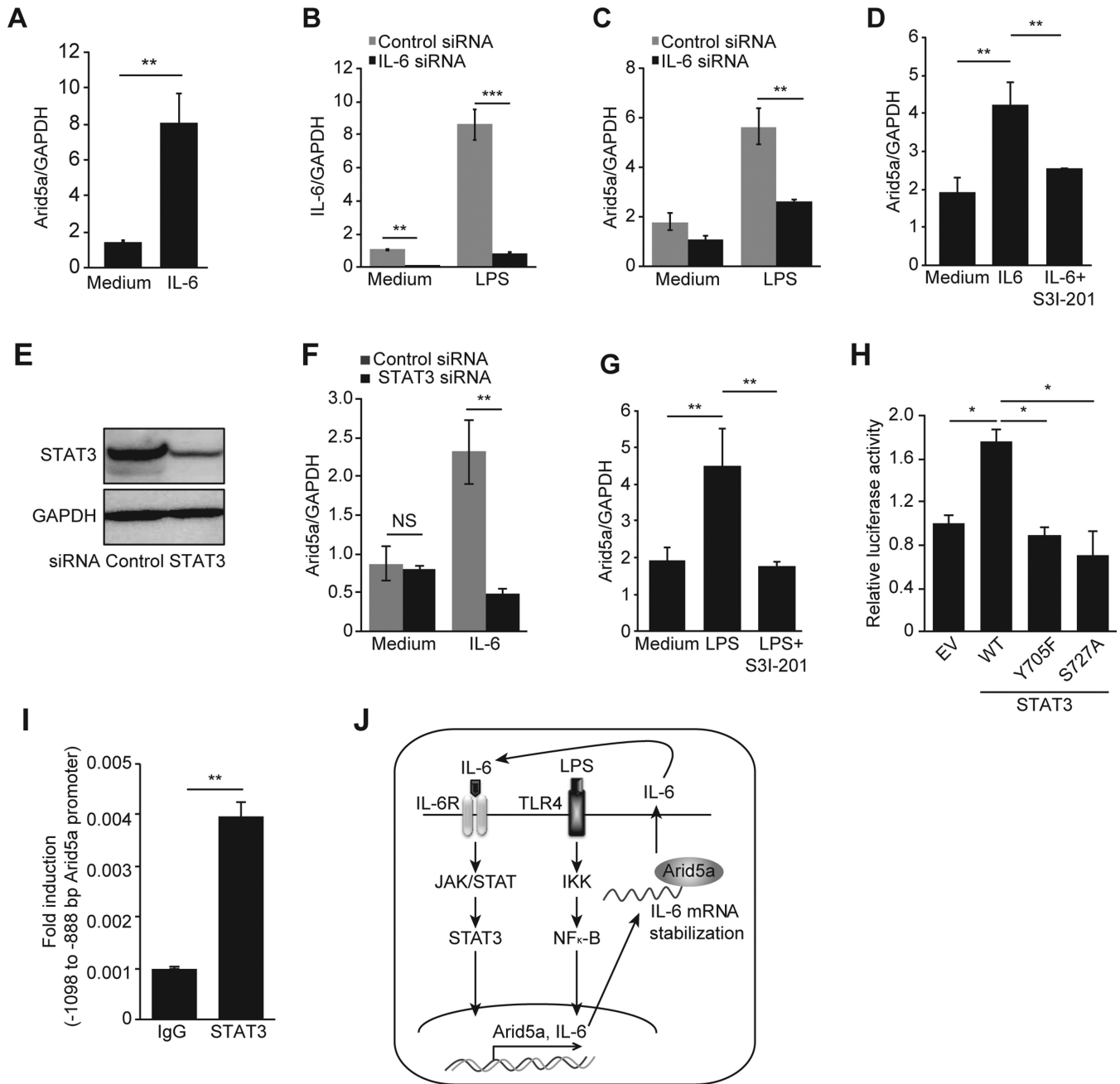


Figure 2. IL-6 stimulates the expression of Arid5a via STAT3 in response to LPS. (A) Arid5a mRNA expression was measured using qPCR in MEFs stimulated with IL-6 (35 ng/ml) for 1 h. (B) IL-6 mRNA expression was knocked down in MEF cells using an IL-6 siRNA followed by stimulation with LPS (10 μg/ml). (C) Expression of Arid5a in LPS-stimulated knockdown MEF cells (10 μg/ml) for 1 h. (D) Expression of Arid5a mRNA in MEFs that were pretreated with a Stat3 inhibitor (50 μM) or DMSO (control) for 45 min and then stimulated with IL-6 (35 ng/ml) for 1 h. (E) Immunoblot assays of Stat3 expression in MEFs transfected with 20 nM control or Stat3 siRNA. (F) Arid5a mRNA expression in the control and Stat3 knockdown MEFs after stimulation with IL-6 (35 ng/ml). (G) Expression of Arid5a mRNA in MEFs that were pretreated with a Stat3 inhibitor (50 μM) or DMSO (control) for 45 min and then stimulated with LPS (10 μg/ml) for 1 h. (H) Luciferase activity of the Arid5a promoter was determined as described above in 1E in combination with the empty vector or WT Stat3 and its phosphorylation site mutants (Y705F and S727A) expression vectors. (I) ChIP assay was performed as described above in 1G using LPS stimulated-macrophages, and chromatin was immunoprecipitated with anti-Stat3 antibody and anti-IgG (negative control). (J) Schematic diagram illustrating the mechanism proposed in this study, in which the TLR4/IKK/NF-κB and IL-6/STAT3 signaling pathways transcriptionally regulate Arid5a gene expression. During LPS signaling, NF-κB upregulates Arid5a, which in turn increases the production of IL-6 by stabilizing its mRNA. IL-6 further stimulates the expression of Arid5a and IL-6 via a positive feedback loop. The values are shown relative to normalized levels after cells were transfected using an empty vector. All data are shown the mean ± SD of three independent experiments. Error bars indicate the mean ± SD. NS, not significant; **P* < 0.05; ***P* < 0.01; ****P* < 0.001.

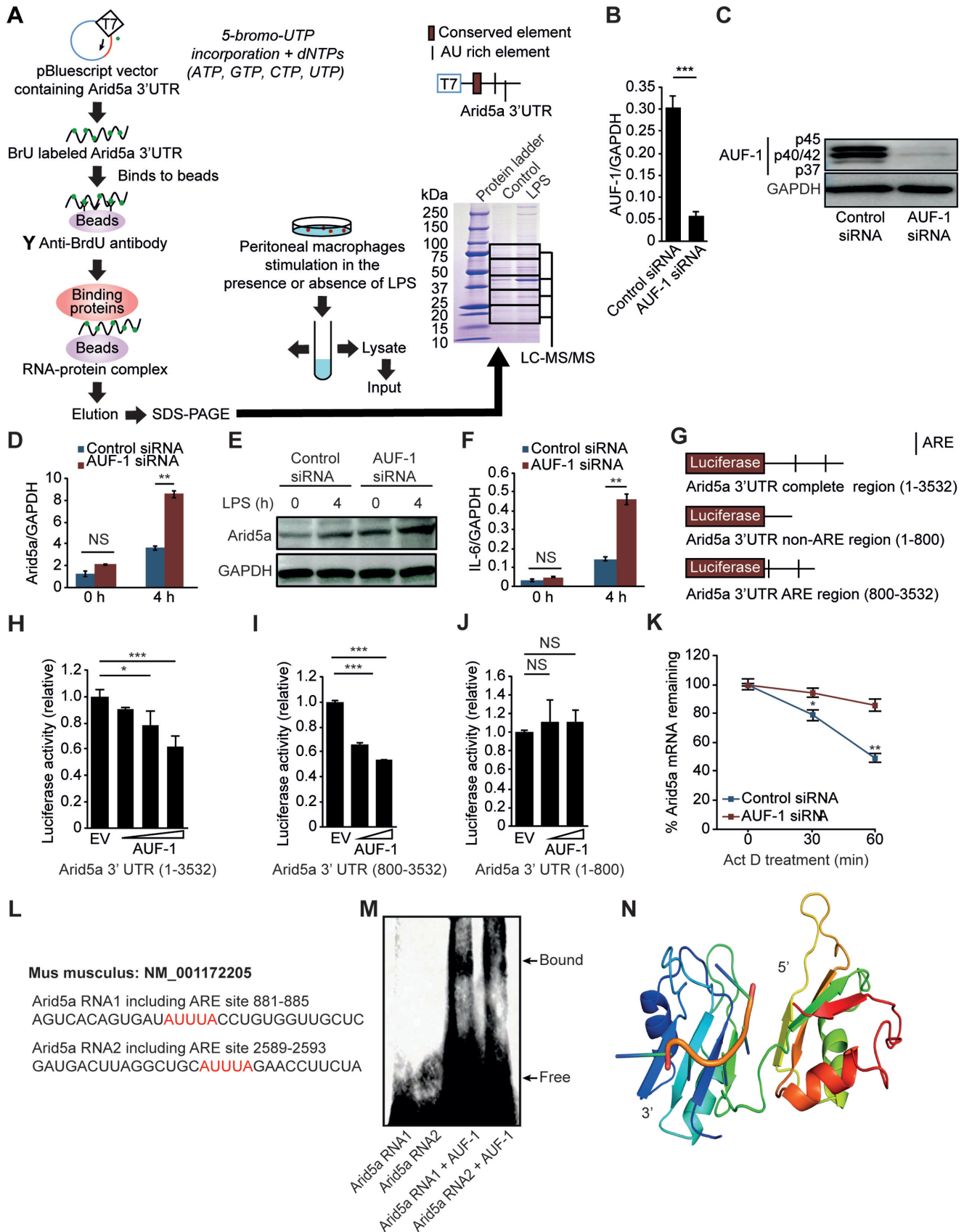


Figure 3. AUF-1 destabilizes the Arid5a mRNA by recognizing the Arid5a 3' UTR. (A) Identification of the RNA-binding protein AUF-1 on the Arid5a 3' UTR. Peritoneal macrophages were stimulated with or without LPS (1 μ g/ml) for 4 h. Whole-cell lysates were then obtained and mixed with binding

ther contained (~2.7 kb) or did not contain (~810 bp) its 3' UTR ARE sites (Figure 3G). Cells were also transfected with an AUF-1 expression construct. Overexpressing AUF-1 decreased luciferase activity more when cells were transfected with the pGL3 vector that encoded the Arid5a 3' UTR containing the ARE region than that when cells were transfected with the luciferase vector alone (Figure 3H–I). In contrast, overexpressing AUF-1 did not affect the luciferase activity of the pGL3 vector that encoded the Arid5a 3' UTR without its ARE region (Figure 3J), suggesting that AUF-1 binds to the ARE region of the Arid5a mRNA and that this binding process may be involved in destabilizing the Arid5a mRNA.

Having identified the likely AUF-1 binding region on Arid5a 3' UTR, we next sought to determine whether AUF-1 contributes to Arid5a mRNA stability. WT and AUF-1 knockdown MEF cells were stimulated first with LPS for 2 h and then treated with Actinomycin D. The half-life of Arid5a mRNA was significantly longer in AUF-1 knockdown MEF cells than that in their WT counterparts (Figure 3K). Because there are 2 ARE regions in the Arid5a 3' UTR (Figure 3L), we designed two short biotinylated RNA sequences (RNA1 and RNA2) that surrounded these ARE regions and performed RNA-EMSA to confirm our finding that AUF-1 binds to the ARE-containing regions of the Arid5a mRNA (Figure 3M). The results were further validated by an *in silico* docking model, which showed that AUF-1 can physically bind to the ARE region (AUUUA) of the 3' UTR (Figure 3N). Collectively, these results demonstrate that AUF-1 binds to the ARE sites in the 3' UTR region of Arid5a mRNA to destabilize it.

MKP-1 signaling is required for the AUF-1-mediated regulation of Arid5a mRNA stability

MKP-1 was previously reported to promote the translocation of the RBP AUF-1 from the nucleus to the cytoplasm in response to LPS stimulation (11). To determine whether MKP-1 signaling is required for the AUF-1-mediated destabilization of Arid5a mRNA, we generated MKP-1 knockdown MEF cells using MKP-1-specific siRNAs (Figure 4A and B). MKP-1 deficiency did not affect AUF-1 mRNA expression levels (Figure 4C); thus, we then evaluated the subcellular localization of AUF-1 in the cytoplasm and nucleus of these cells compared to that of their WT counterparts upon stimulation with LPS. Our data showed that knockdown of MKP-1 significantly inhibited the translocation of

AUF-1 proteins from the nucleus to the cytoplasm (Figure 4D), consistent with a previous report showing that MKP-1 modulated AUF-1 protein levels during its translocation from the nucleus to the cytoplasm in RAW cells (11).

To determine whether MKP-1 knockdown-mediated inhibition of the cytoplasmic translocation of the AUF-1 protein affected the stability of Arid5a mRNA, we performed an Actinomycin D mRNA stability assay using control and MKP-1 knockdown MEF cell lines. We found that Arid5a mRNA degradation was significantly slower in the MKP-1 knockdown MEF cells than that in their control counterparts (Figure 4E). Additionally, the mRNA expression levels of Arid5a and IL-6 were higher in the MKP-1-deficient MEFs than those in the control cells (Figure 4F and G). Thus, these data suggest that LPS signaling drives MKP-1 to increase the shuttling of AUF-1 from the nucleus to the cytoplasm, where it binds to the 3' UTR region of Arid5a mRNA to destabilize it (Figure 4H).

Arid5a is phosphorylated by p38 MAP kinase

After 4 h of LPS treatment, Arid5a protein expression gradually decreased and was almost abolished within 24 h (Figure 1B). This observation prompted us to investigate the post-translational signaling pathways that regulate the observed decrease in Arid5a protein expression. To determine whether Arid5a is phosphorylated as a result of the activation of TLR4 signaling, we transfected HEK293TLR4 cells with a Flag-Arid5a expression vector and then stimulated the cells with LPS. Whole-cell lysates were then immunoprecipitated using Flag and normal IgG (as control) antibodies and subjected to SDS-PAGE. Bands located at the predicted position of Arid5a according to CBB staining were cut out and analyzed using LC-MS/MS (Figure 5A). The MS data indicated that serines at positions 253, 433 and 458 of the Arid5a protein were phosphorylated in response to TLR4 signaling (Figure 5B and C). Furthermore, the phosphorylation of mouse Arid5a was reduced when constructs in which the serine residues located at Ser253, Ser433 and Ser458 were substituted with alanine (S253A, S433A and S458A, respectively) were transfected into HEK293TLR4 cells (Figure 5D and E). These data indicated that these three Arid5a serine residues are targeted for phosphorylation in response to LPS signaling, further confirming the data obtained from LC-MS/MS. Additionally, when Arid5a-deficient MEF cells were transfected with Flag-Arid5a and then transfected with or without LPS, the

protein G beads in solution with the Arid5a 3' UTR (containing BrdU), and the eluted buffer was then subjected to SDS-PAGE. The gel that was run using the complex containing the Arid5a 3' UTR and beads was stained using CBB after SDS-PAGE and then separated into five compartments that were independently analyzed using LC-MS/MS. (B and C) Analysis of AUF-1 mRNA and protein levels in MEF cells that were transfected with control siRNA or AUF-1 siRNA. (D–F) Arid5a mRNA (D) and protein expression (E) and IL-6 mRNA expression (F) in the control and AUF-1 knockdown MEF cells at 4 h after stimulation with LPS (5 µg/ml). (G) Diagram of the region of the pGL3 vector that encodes the Arid5a 3' UTR (1–3532), Arid5a 3' UTR (1–800), or Arid5a 3' UTR (800–3532). The black bar shows the locations of AU-rich elements (AREs). (H–J) The luciferase activities of each of the vectors that encodes one of three different fragments of the Arid5a 3' UTR are shown in G. The results were obtained using MEF cells that were transfected for 48 h with an AUF-1 expression vector or an empty vector. (K) Quantitative real-time PCR analysis of the Arid5a mRNA in the control and AUF-1 knockdown MEFs that were stimulated for 2 h with LPS (3 µg/ml). The cells were then treated for 0–60 min with Actinomycin D. (L) A predicted ARE region in the Arid5a 3' UTR is shown in red. (M) Electrophoretic mobility shift assay (EMSA) demonstrating the interaction between the AUF-1 recombinant protein and 3'-biotinylated fragments with the Arid5a 3' UTR, as shown in L. (N) Putative binding mode of mouse AUF-1 protein with the homology model of AUF-1 shown as a cartoon with rainbow colors from N (blue) and to C (red). The AUUUA RNA fragment from PDB entry 1g2e is shown as an orange cartoon with light green residues in stick representation and with the flexibly docked RNA models shown as orange backbone traces. All data are shown as the mean ± SD of three independent experiments. Error bars indicate the mean ± SD. **P* < 0.05; ***P* < 0.01; ****P* < 0.001.

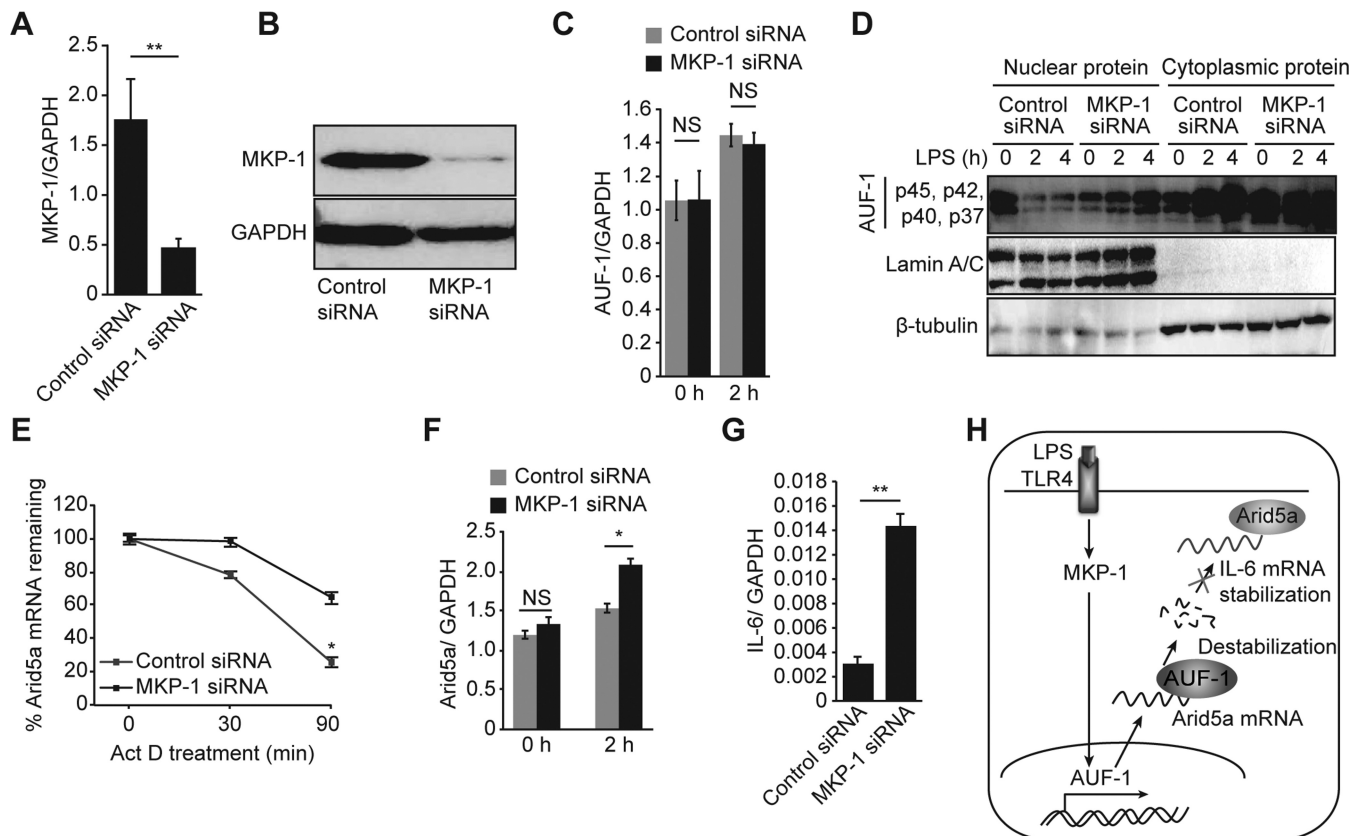


Figure 4. MKP-1 signaling regulates Arid5a mRNA stability by inducing the translocation of AUF-1 from the nucleus to the cytoplasm. (A and B) Analysis of MKP-1 mRNA and protein levels in MEF cells that were transfected with control siRNA and MKP-1 siRNA. (C) Quantitative real-time PCR analysis of AUF-1 mRNA levels in control and MKP-1 knockdown cells that were stimulated with LPS (3 μ g/ml). (D) AUF-1 (p45, p42, p40, p37) levels in the cytoplasm versus the nucleus in control and MKP-1 knockdown MEF cells that were stimulated using LPS for 0–4 h. β -tubulin and Lamin A/C were used as the loading controls for cytoplasmic proteins and nuclear proteins, respectively. (E) Quantitative real-time PCR analysis of mRNA levels of Arid5a in control and MKP-1 knockdown MEFs that were stimulated with LPS and then treated with Actinomycin D for 0–90 min. (F and G) Quantitative real-time PCR analysis of mRNA levels of Arid5a and IL-6 in control and MKP-1 knockdown MEFs that were stimulated with LPS. (H) Schematic diagram illustrating the post-transcriptional regulation of Arid5a mRNA. LPS signaling induces MKP-1, which in turn signals AUF-1 to translocate from the nucleus to the cytoplasm. In the cytoplasm, AUF-1 binds to AU-rich elements on the Arid5a 3' UTR to destabilize the Arid5a mRNA. This results in the inhibition of the stabilization of the IL-6 mRNA. All data are shown as the mean \pm SD of three independent experiments. N.S., not significant. * P < 0.05; ** P < 0.01.

results were consistent with similar experiments performed using HEK293TLR4 cells (Supplementary Figure S1). Notably, sequencing analysis showed that these sites were conserved across species ranging from mice to humans (Figure 5F).

Because we showed that exposing the TLR4 receptor to LPS results in the activation of two major kinase-mediated signaling pathways, including the MAPK and IKK complexes, we next sought to determine which kinase(s) are involved in the phosphorylation of Arid5a in response to LPS signaling. Therefore, we overexpressed different kinases in HEK293TLR4 cells to explore the effects on downstream TLR4 signaling. Interestingly, we found that p38 MAP kinase interacted with and phosphorylated Arid5a proteins (Figure 5G). Although IKK α and IKK β were also shown to interact with Arid5a, neither was able to phosphorylate Arid5a (Figure 5G). Collectively, these results indicated that the p38 MAP kinase phosphorylates Arid5a at its serine amino acids via a TLR4 signaling-mediated mechanism during the late phase response to stimulation with LPS.

Phosphorylation-associated ubiquitination of Arid5a by p38

Phosphorylation of proteins is sometimes associated with ubiquitination, which generally results in degradation. Therefore, to investigate the mechanism by which Arid5a is ubiquitinated, we expressed WT Flag-Arid5a and HA-tagged ubiquitin in HEK293TLR4 cells in addition to several kinases known to be involved in the ubiquitination process, including IKK α , IKK β , IRAK1, IKK ϵ and p38 MAPK. We observed that co-expressing p38 with ubiquitin and Arid5a resulted in significant degradation/ubiquitination of Arid5a, suggesting that p38 mediates the ubiquitination of Arid5a (Figure 6A). Next, to determine whether the ubiquitination of Arid5a is associated with its phosphorylation, we performed ubiquitination assays in which we overexpressed WT Arid5a or Arid5a that was mutated at S253A, S433A and S458A with p38 in HEK293TLR4 cells. Whereas WT Arid5a underwent ubiquitination in response to p38, the mutant form of Arid5a (at S253A, S433A and S458A) did not (Figure 6B), suggesting that the phosphorylation of Arid5a promotes its

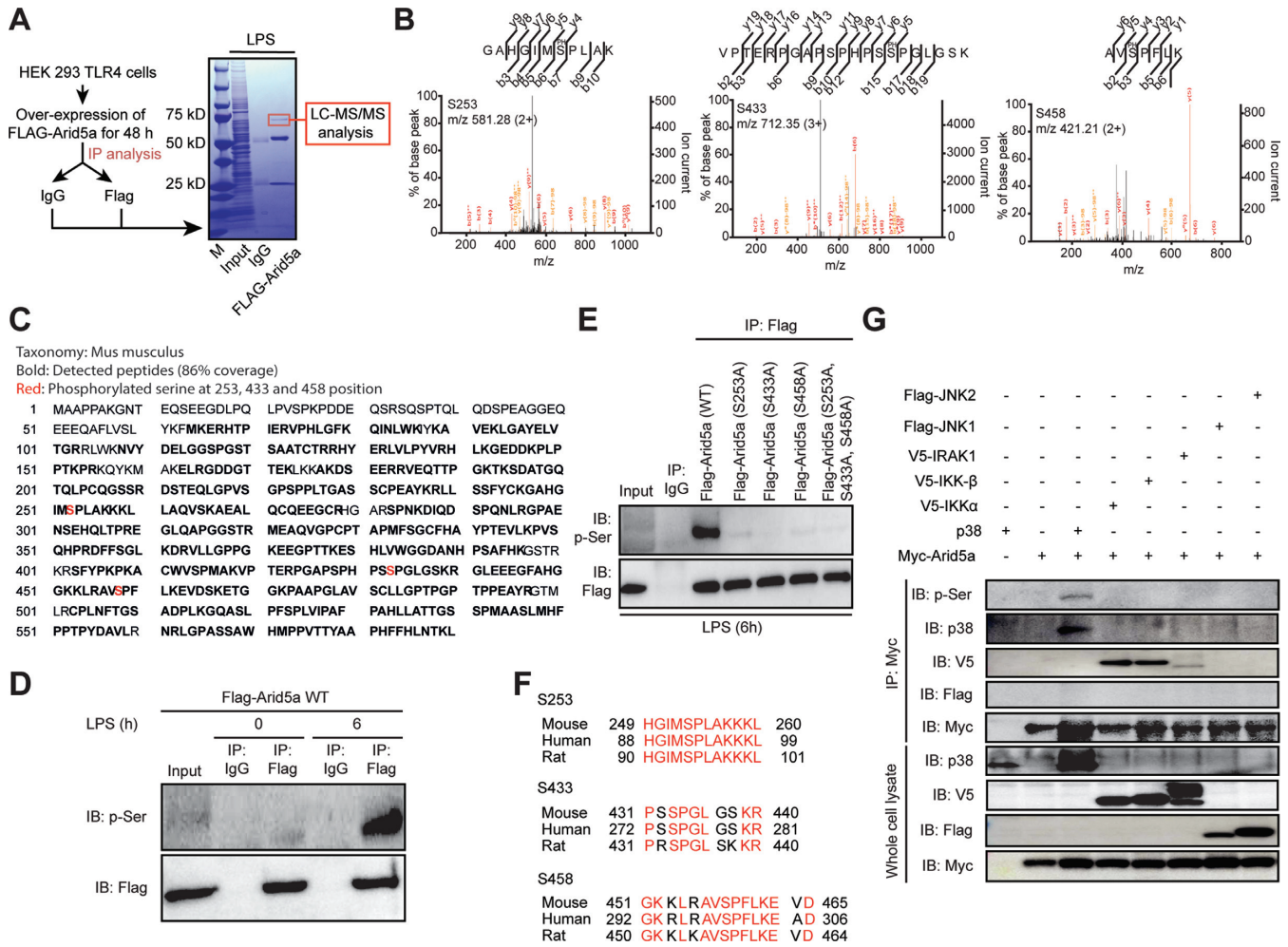


Figure 5. p38 MAPK is essential for Arid5a phosphorylation. (A) Identification of unique phosphorylation sites in the Arid5a protein. HEK293TLR4 cells overexpressing a Flag-Arid5a expression vector (2 μg) for 48 h were then stimulated with LPS (1 μg/ml) for 0 or 6 h. Whole-cell lysates were equally divided and then immunoprecipitated with normal IgG and anti-Flag antibodies in the presence of a phosphatase inhibitor. They were then mixed with protein G beads and eluted. The elution buffers were subjected to SDS-PAGE. The gel was stained using CBB, and the Arid5a region was cut from the gel for analysis using LC-MS/MS. (B) The calculated target ions for serine 253 (left panel), serine 433 (middle panel) and serine 458 (right panel) are shown. (C) The peptides (bold) corresponding to the mouse Arid5a protein were detected. The MS/MS spectra were analyzed using a Mascot Server (Matrix Science). The positions of the phosphorylation sites (red color) in the mouse Arid5a protein (590 aa) were analyzed using mass spectrometry. (D and E) Immunoblot analysis of phosphorylated Arid5a in HEK293TLR4 cells that were transfected with WT and S253A, S433A and S458A-mutant Flag-Arid5a and then stimulated for 0 or 6 h with LPS. The mixtures were then immunoprecipitated to obtain the proteins of interest (Arid5a and its mutant form) from the lysates using anti-Flag and anti-normal IgG and an immunoblot analysis of phosphoserine (with anti-p-Ser) and Arid5a (with anti-Flag). (F) Alignment of phosphorylation sites in the Arid5a protein between humans, mice and rats. The region shown in red indicates the conserved amino acids. (G) Immunoblot analysis of the phosphorylation of Arid5a in HEK293TLR4 cells after it was allowed to interact with several kinases following transfection with WT Myc-Arid5a, V5-IKKα, V5-IKKβ, V5-IRAK1, p38, Flag-JNK-1 and Flag-JNK-2 expression vectors. The cell lysates were prepared and immunoprecipitated to obtain the Arid5a protein using anti-Myc antibodies. This was followed by an immunoblot analysis of Arid5a (with anti-Myc antibodies), p38 (with anti-p38 antibodies), IKKα/β/IRAK1 (with anti-v5 antibodies), JNK-1/2 (with anti-Flag antibodies) and phosphoserine (with anti-p-Ser antibodies). Below, immunoblots of whole cell lysates that were treated with anti-v5, anti-p38, anti-Flag or anti-Myc antibodies. The data are representative of two–three independent experiments.

ubiquitination. To determine whether Arid5a is ubiquitinated in response to LPS-induced signaling, we performed a ubiquitination assay on Arid5a in mixtures treated with or without LPS. As expected, Arid5a was ubiquitinated 6 h after LPS stimulation (Figure 6C). Next, to determine the sites on Arid5a that are required for its ubiquitination, we performed LC-MS/MS of Arid5a that had been immunoprecipitated in the presence or absence of p38. The results showed that Arid5a was ubiquitinated at lysines 80 and 89 (Figure 6D–F). The ubiquitination of Arid5a was re-

duced when these lysine residues were substituted with arginine (K80R, K89R), indicating that these two Arid5a lysine residues were targeted for ubiquitination by p38 MAP kinase (Figure 6G).

WWP1 E3 ligase ubiquitinates Arid5a and controls IL-6 levels

Having confirmed that LPS-induced phosphorylation of Arid5a by p38 is associated with ubiquitination, we next investigated which E3 ligase is required for the ubiquiti-

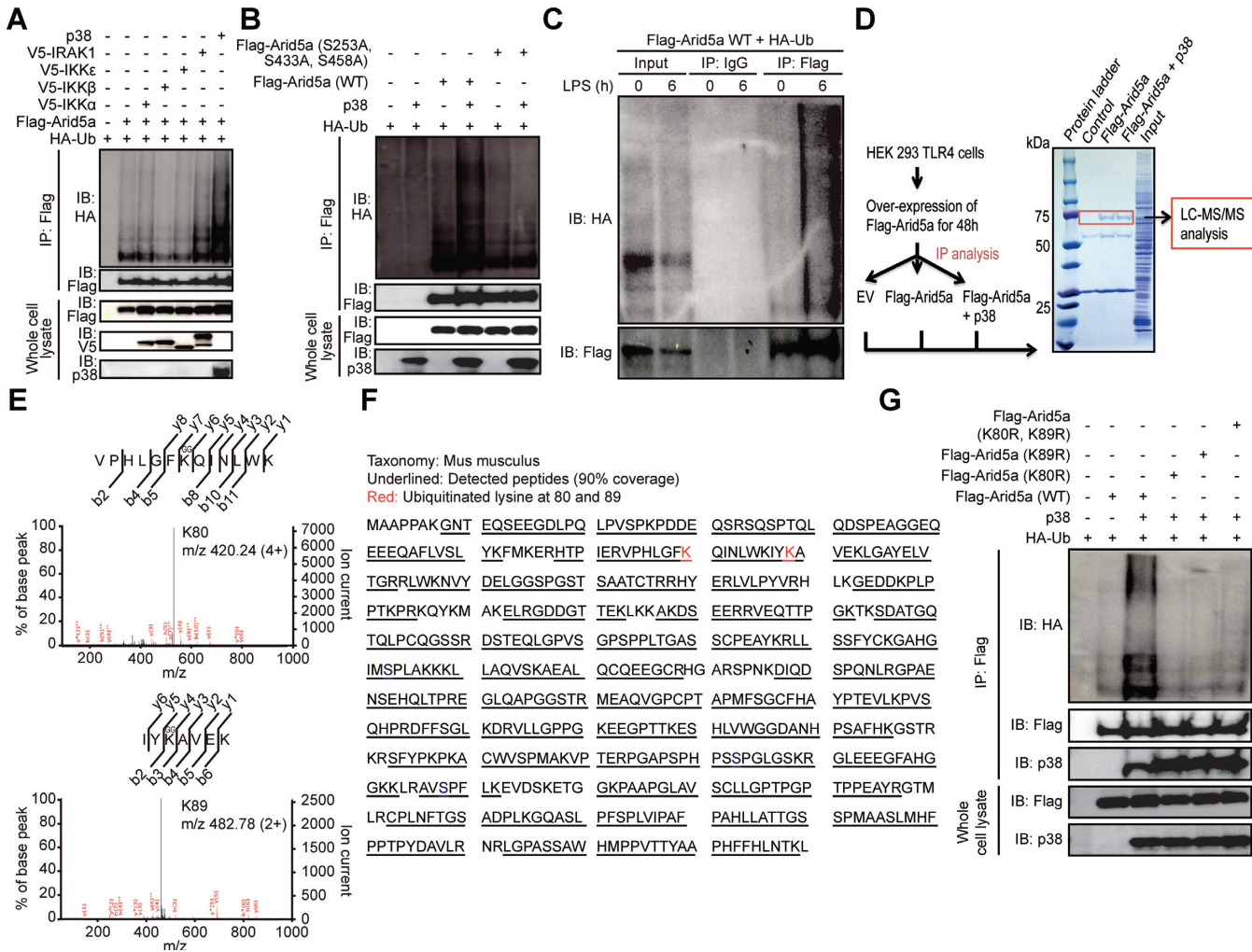


Figure 6. Arid5a is ubiquitinated in response to TLR4-p38 signaling. (A) Arid5a is ubiquitinated by p38. HEK293TLR4 cells were transfected with hemagglutinin-tagged ubiquitin (HA-Ub), Flag-tagged Arid5a and/or the v5-IKK α , v5-IKK β , v5-IKK ϵ , v5-IRAK1 or p38 expression vector (as indicated above the lanes). Cell lysates were then immunoprecipitated in the presence of MG-132 (1 μ M) using anti-Flag antibodies and submitted to an immunoblot analysis of ubiquitin (using anti-HA antibodies) and Arid5a (using anti-Flag antibodies). Below, immunoblots of whole-cell lysates treated with anti-v5, anti-p38 or anti-Flag antibodies. (B) Ubiquitination is impaired in the Arid5a phosphorylation mutant. HEK293TLR4 cells were transfected to express HA-Ub, Flag-tagged Arid5a (WT), S253A, S433A and S458A-mutant Flag-Arid5a and/or a p38 expression vector (as indicated above the lanes). The lysates were then immunoprecipitated in the presence of MG-132 (1 μ M) using anti-Flag antibodies and submitted to immunoblot analysis for ubiquitin (using anti-HA antibodies) and Arid5a (using anti-Flag antibodies). Below, an immunoblot of whole cell lysates that was performed using anti-p38 or anti-Flag antibodies is shown. (C) LPS stimulation induces the ubiquitination of Arid5a. Arid5a-deficient MEFs overexpressed WT Flag-Arid5a and hemagglutinin-tagged ubiquitin. The cells were then stimulated with LPS (10 μ g/ml) for the indicated times and subsequently immunoprecipitated with Flag and IgG (control) antibodies in the presence of a proteasome inhibitor (MG-132; 1 μ M) and analyzed by anti-HA (upper) and anti-Flag (below) antibodies for ubiquitin and Arid5a, respectively. (D–F) Detection of ubiquitination sites in the mouse Arid5a protein using LC-MS/MS analysis. HEK293TLR4 cells were transfected with expression vectors encoding Flag-Arid5a either alone or with p38 and empty vectors. The cells were then treated with MG-132 (1 μ M). Flag-Arid5a was immunoprecipitated using Flag, and the eluted samples were subjected to SDS-PAGE. Bands were analyzed using mass spectrometry (D). The calculated target ions for lysine 80 (left panel) and lysine 89 (right panel) are shown (E). The peptides (underlined) corresponding to the mouse Arid5a protein were detected. The positions of the identified ubiquitination sites (red color) in the mouse Arid5a protein sequence (590 aa), as determined using mass spectrometry (F). (G) Ubiquitination of Arid5a is impaired in Arid5a ubiquitination site mutants. HEK293TLR4 cells were transfected with expression vectors containing WT Flag-Arid5a, K80R and K89R mutant Arid5a, or p38 and HA-Ub and then immunoprecipitated using Flag in the presence of MG-132 (1 μ M). Immunoblot analyses were performed for ubiquitin (using anti-HA antibodies), Arid5a (using anti-Flag antibodies) and p38 (using anti-p38 antibodies). Below, an immunoblot of whole-cell lysates that was performed using anti-Flag and anti-p38 antibodies is shown. The data are representative of two or three independent experiments.

nation of Arid5a. Therefore, we screened several TLR4-activated E3 ubiquitin ligases as possible candidates responsible for the ubiquitination of Arid5a using siRNA inhibition in MEF cells followed by LPS stimulation (Figure 7A and B; Supplementary Figure S2A–D). Of these, WWP1-knockdown MEFs failed to ubiquitinate Arid5a in response to LPS (Figure 7B), suggesting that WWP1 acts as an E3 ligase of Arid5a in the TLR4 signaling pathway. In the co-immunoprecipitation assay, WWP1 was also shown to be immunoprecipitated with Arid5a (Figure 7C) and p38 (Figure 7D), suggesting that Arid5a, WWP1 and p38 interact with each other and likely form a complex. To further confirm our hypothesis, we next performed an ubiquitination assay of Arid5a by overexpressing HA-Ub, Flag-tagged WWP1 and Myc-tagged Arid5a in HEK293TLR4 cells and then immunoprecipitated the proteins with an anti-Myc antibody. We observed that over-expression of WWP1 resulted in significant ubiquitination of Arid5a (Figure 7E).

Since Arid5a is known to regulate the expression of IL-6 by stabilizing its mRNA, we next determined the effect of WWP1 on IL-6 through knockdown of endogenous WWP1 by RNA interference in MEFs. Depletion of WWP1 resulted in significant augmentation of IL-6 in response to LPS (Figure 7F), suggesting that WWP1-mediated ubiquitination of Arid5a affects the stabilization of IL-6 via the TLR4 signaling pathway. Collectively, WWP1 interacts with p38 and Arid5a and induces the ubiquitination of Arid5a under TLR4 signaling.

Phosphorylation-mediated degradation of Arid5a by p38 controls IL-6 expression

The phosphorylation of the RBP Regnase-1 led to its degradation by TLR or IL-1R signaling (8). Because Arid5a has been shown to counteract the activity of Regnase-1, we therefore sought to confirm whether the phosphorylation of Arid5a also resulted in its degradation. We expressed Flag-tagged WT Arid5a or Arid5a constructs containing mutations at S253A, S433A and S458A in Arid5a-deficient MEFs and then stimulated the cells with LPS. Whereas WT Arid5a was degraded in response to LPS stimulation, the S253A, S433A and S458A mutants were resistant/less affected by this stimulus (Figure 8A). These results were confirmed using densitometry analyses of the blots (Figure 8B).

We observed that p38 induced the phosphorylation of Arid5a in response to LPS (Figure 5). To determine whether p38/TLR4 signaling is responsible for the degradation of Arid5a, we knocked down p38 in MEF cells using p38-specific siRNA (Figure 8C) and measured the Arid5a mRNA expression after LPS stimulation. The knockdown of p38 did not have significant effects on Arid5a mRNA expression (Supplementary Figure S3) as previously shown in Figure 1C using a pharmacological inhibitor of p38, SB203580. However, when p38 knockdown cells were subsequently transfected with Flag-tagged-Arid5a (WT) and stimulated with LPS, Arid5a protein degradation was reduced in comparison to cells transfected with control siRNAs. Inhibiting p38 reduced the degradation of Arid5a (Figure 8D and E), suggesting that p38 signaling is required to degrade Arid5a.

Our data suggested that phosphorylation of Arid5a is followed by degradation in response to p38/TLR4 signaling. K48-linked ubiquitination is known to be involved in proteasomal degradation. Therefore, we transfected HEK293TLR4 cells with Myc-tagged Arid5a, HA-tagged ubiquitin, K48-HA-tagged ubiquitin and p38 and then immunoprecipitated proteins with anti-Myc. We found Arid5a was similarly ubiquitinated in the presence of K48-HA-Ub as in WT HA-Ub (Figure 8F), suggesting that p38 degraded Arid5a through K48-linked ubiquitination by recruiting WWP1.

Because Arid5a stabilizes the IL-6 mRNA, resulting in increased levels of IL-6 after LPS challenge (7), we sought to determine the effect of the phosphorylation-mediated degradation of Arid5a on expression of the IL-6 mRNA. Interestingly, when cells were stimulated with LPS, IL-6 mRNA expression was significantly higher in MEF cells transfected with the S253A, S433A and S458A mutant Arid5a than that in cells transfected with WT Arid5a (Figure 8G). These results were further supported by IL-6 3' UTR luciferase assays that showed increased activity at the IL-6 3' UTR when HEK293 cells were transfected with S253A, S433A or S458A mutant Arid5a than that in cells transfected with WT Arid5a (Supplementary Figure S4). Collectively, these results indicated that p38 MAP kinase mediates the phosphorylation of Arid5a, inducing its ubiquitination and degradation during the late phase following LPS stimulation. However, mutating specific phosphorylation sites in Arid5a inhibited its degradation, resulting in overproduction of IL-6 (Figure 8H).

DISCUSSION

In this study, we identified the signaling pathways through which Arid5a regulates IL-6 mRNA stability. First, we showed that TLR4 induces *Arid5a* gene expression via an IKK-mediated NF- κ B signaling mechanism. In parallel to this process, *Arid5a* gene expression is also activated by IL-6-mediated STAT3 signaling, which acts synergistically with LPS signaling. Furthermore, the RBP AUF-1 binds to the Arid5a mRNA 3' UTR to destabilize it, and this involves a MKP-1-mediated mechanism. Arid5a is phosphorylated by MAPK-activated p38 during the late phase of TLR4 stimulation, leading to its degradation through WWP1 E3 ubiquitin ligase via a ubiquitin–proteasome-dependent mechanism. Significantly, Arid5a mutant proteins that were resistant to degradation demonstrated increased potency, which overwhelmed the expression of IL-6. Thus, regulation of the expression and degradation of Arid5a by TLR4-activated NF- κ B and MAPK signaling mechanisms results in the amplification of IL-6 expression, triggering further inflammation.

NF- κ B family transcription factors consist of homo- and heterodimers that include the Rel family members, p50 p52, p65, RelB and c-Rel. Among these, p65, RelB and c-Rel are transcriptionally active members of the NF- κ B family, whereas p50 and p52 function primarily as non-transactivating DNA-binding subunits (26). Here, we further validated the contribution of the p65 and c-Rel subunits of NF- κ B in transcriptionally inducing the *Arid5a* gene in the early phase of TLR4 stimulation. Our data sug-

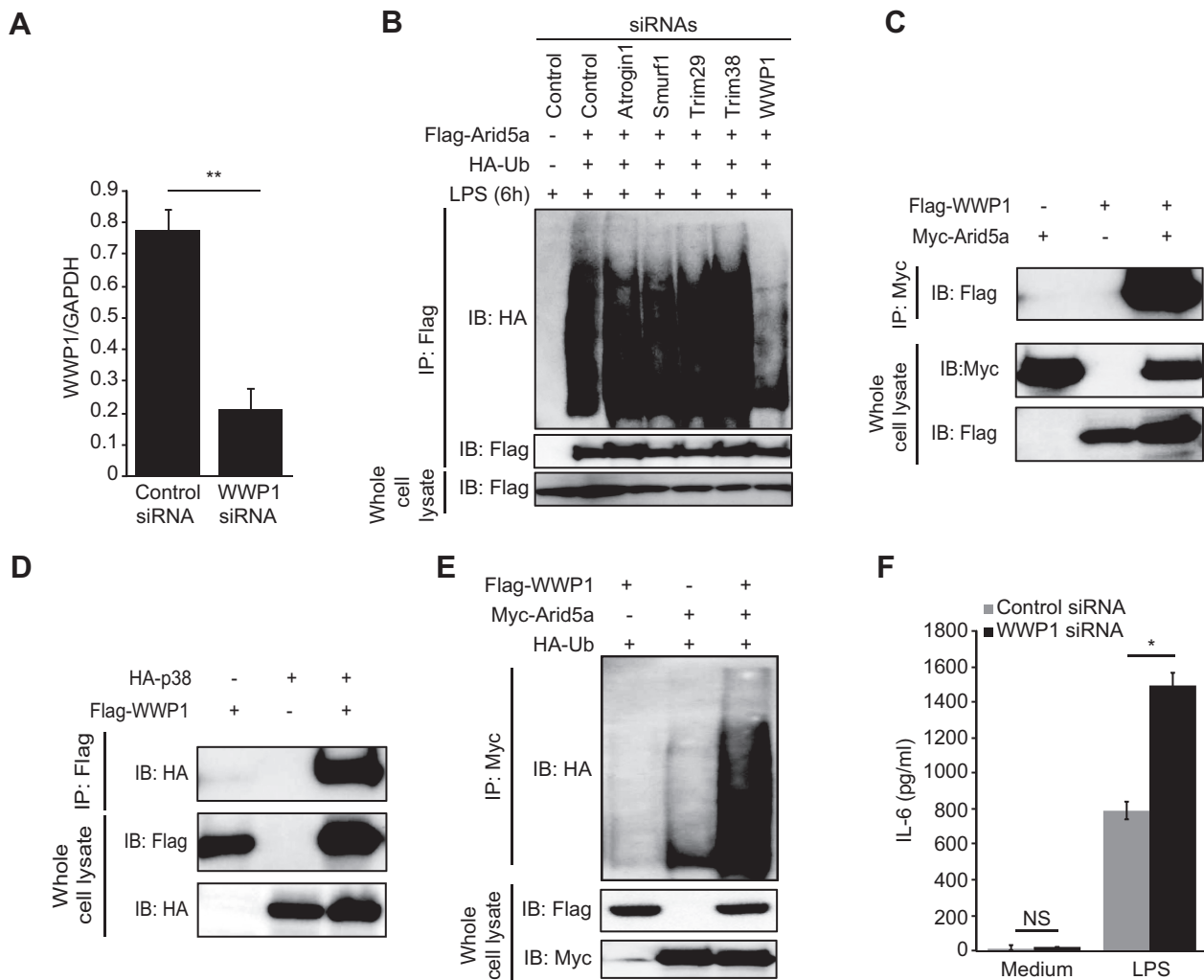


Figure 7. WWP1 E3 ubiquitin ligase mediates Arid5a polyubiquitination. (A) Analysis of WWP1 mRNA expression in MEF cells that were transfected with control siRNA and WWP1 siRNA (20 nM each). (B) MEF cells were treated with 20 nM control and E3 ubiquitin ligase siRNAs (WWP1, Atrogin1, Trim29, Trim38 and Smurf1) for 72 h and transfected to express hemagglutinin-tagged ubiquitin (HA-Ub) and Flag-tagged Arid5a (as indicated above the lanes). The cells were then stimulated for 6 h with LPS (10 μ g/ml) and incubated for 6 h with MG-132 (1 μ M) followed by immunoprecipitation with anti-Flag antibodies and immunoblot analyses of ubiquitin (using anti-HA) and Arid5a (using anti-Flag). Below, immunoblots of whole-cell lysates treated with anti-Flag antibody. (C and D) Immunoblot analysis of molecular interactions in HEK293TLR4 cells following transfection for 48 h with WT Myc-Arid5a, Flag-WWP1 (C) and HA-p38, Flag-WWP1 (D). The lysates were immunoprecipitated using anti-Myc (C) and anti-Flag (D) antibodies. This was followed by an immunoblot analysis of WWP1 (with anti-Flag antibody), p38 (with anti-HA antibody). Below, immunoblots of whole-cell lysates that were treated with anti-Myc, anti-Flag (C) and anti-HA, anti-Flag (D) antibodies. (E) Immunoassays of HEK293TLR4 cells transfected for 48 h to express HA-tagged Ub, Myc-tagged Arid5a or Flag-tagged WWP1 expression vector (as indicated above the lanes), then incubated for 6 h with MG-132 (1 μ M) followed by immunoprecipitation with anti-Myc antibodies and immunoblot analyses of ubiquitin (using anti-HA). Below, immunoblots of whole-cell lysates treated with anti-Flag or anti-Myc antibodies. (F) IL-6 protein levels in the supernatants of control and WWP1 knockdown MEF cells at 24 h after stimulation with LPS (10 μ g/ml). The data are representative of two–three independent experiments.

gest that IKK-mediated NF- κ B signaling is the key regulator of *Arid5a* gene expression. Hence, there is value in further deciphering the molecular mechanisms underlying the transcriptional control of the *Arid5a* gene by IKK signaling in inflammatory and autoimmune diseases.

IL-6/STAT3 signaling was previously shown to induce IL-6 via autocrine stimulation (27), and STAT3 was previously found to be important for activating *Arid5a* expression in Th17 cells (28). Consistent with these previous studies, we found that IL-6/STAT3 signaling acted synergistically with LPS signaling to activate *Arid5a* expression in MEF cells, suggesting that *Arid5a* expression is regulated

by IL-6 through a positive feedback loop that is itself regulated by TLR4 signaling.

RNA-binding proteins specifically bind to ARE regions in the 3' UTR of mRNAs. RBPs shuttle between the cytoplasm and the nucleus and regulate a variety of cellular processes, such as RNA splicing, export, decay and translation (11). AUF-1 has been shown to recognize stem-loop structures and AREs on the 3' UTR of mRNA (25). Yu *et al.* showed in 2011 that MKP-1 promoted the translocation of AUF-1 from the nucleus to the cytoplasm in response to LPS stimulation and that AUF-1 subsequently bound to various cytokine mRNAs, including IL-6, IL-10

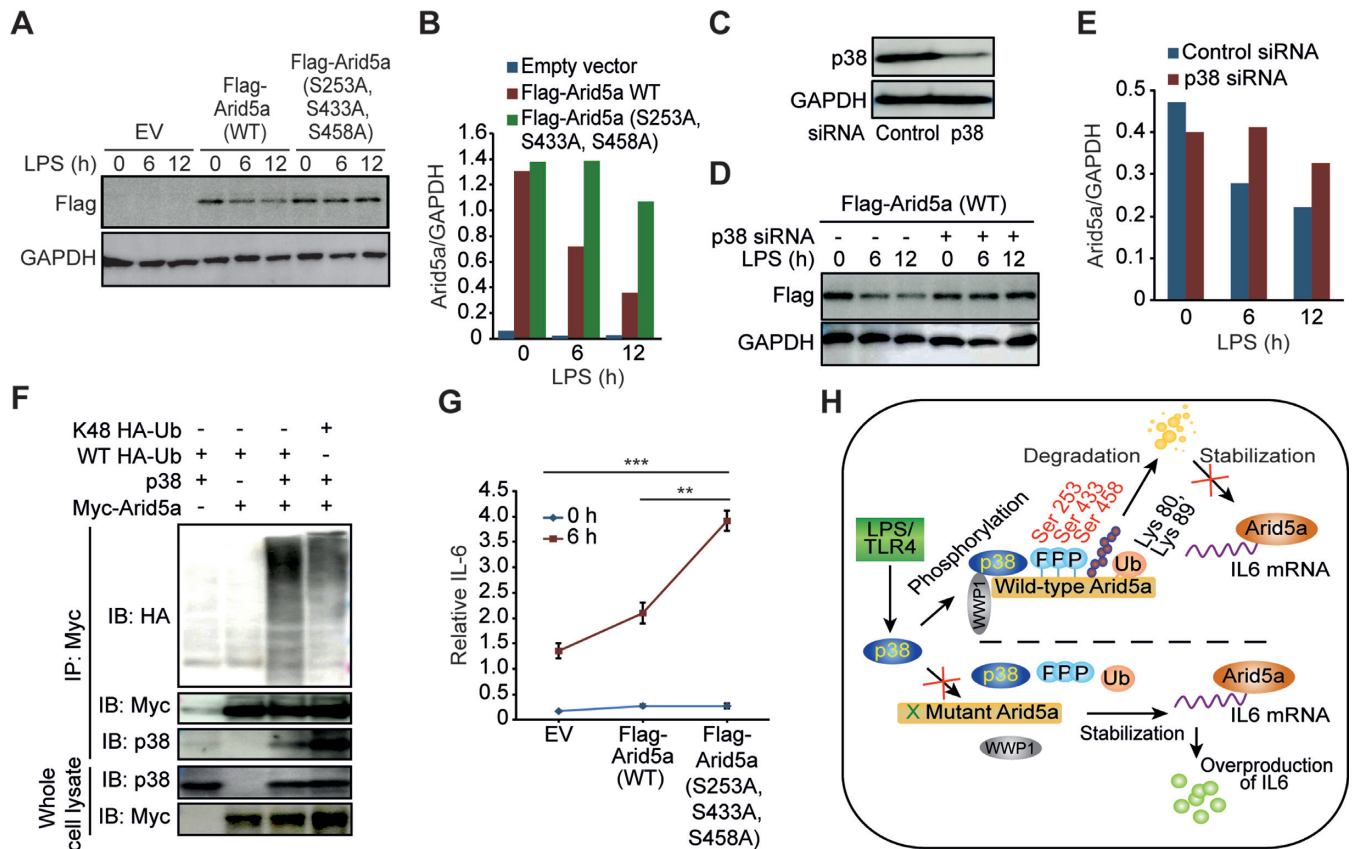


Figure 8. The phosphorylation-mediated degradation of Arid5a affects IL-6 mRNA expression. (A) Immunoblot analysis of lysates obtained from Arid5a-deficient MEF cells that expressed an empty vector (EV) or an expression vector containing WT Flag-tagged Arid5a or S253A, S433A and S458A-mutant Flag-Arid5a. The cells were stimulated for 0–12 h (above lane) with LPS (5 μ g/ml) and then probed with anti-Flag or anti-GAPDH antibodies. (B) Densitometry analysis with results presented as the ratio to GAPDH. (C) Immunoblot assay of p38 expression in MEF cells transfected with 20 nM control or p38 siRNA. (D and E) Immunoblot (D) and densitometry analysis (E) of Flag-tagged Arid5a protein expression following LPS stimulation in control and p38 knockdown MEFs as described above in (A and B). (F) Immunoassay of HEK293TLR4 cells transfected for 48 h to express WT HA-tagged ubiquitin (HA-Ub), K48-HA-Ub, Myc-tagged Arid5a or p38 expression vector (as indicated above the lanes), then incubated for 6 h with MG-132 (1 μ M) followed by immunoprecipitation with anti-Myc antibodies and immunoblot analyses of ubiquitin (using anti-HA), p38 (using anti-p38) and Arid5a (using anti-Myc). Below, immunoblots of whole-cell lysates treated with anti-p38 or anti-Myc antibodies. (G) Quantitative PCR analysis of the expression level of IL-6 mRNA in total RNA obtained from the cells described in A and presented relative to the level of GAPDH RNA. (H) Schematic diagram representing the regulatory mechanism proposed by which degradation of Arid5a by p38 signaling regulates the stability of IL-6 mRNA. The activation of p38 by LPS resulted in the phosphorylation of Arid5a at serine residues 253, 433 and 458, which leads to its ubiquitination on lysine residues 80 and 89 and its subsequent degradation. The degradation of Arid5a results in the inhibition of the stabilization of IL-6 mRNA. Mutating Arid5a at the above described phosphorylation sites blocked it from being degraded, which resulted in the overproduction of IL-6 because its mRNA remained stabilized. The cross shown in green indicates the phosphorylation sites that were mutated in Arid5a, and the cross shown in red indicates its inhibited function. The data are representative of two–three independent experiments. Error bars indicate the mean \pm SD. ** P < 0.01; *** P < 0.001.

and TNF- α , to control the stability of their mRNAs (11). Consistent with these earlier observations, our study of the post-transcriptional mechanisms that regulate Arid5a suggests that MKP-1 plays a dominant role and is critical for shuttling AUF-1 from the nucleus to the cytoplasm, where it suppresses Arid5a and IL-6 mRNA expression. Knocking down AUF-1 using AUF-1-specific siRNA in MEFs resulted in higher levels of Arid5a and IL-6 mRNA expression and also delayed the degradation of Arid5a when cells were treated with Actinomycin D. It has been reported that RBP TTP is involved in degrading IL-6 by binding to its 3' UTR at an ARE region during the inactivation of the p38 MAPK pathway in IL-1 β -stimulated MEFs cells (29). Another study by Zhao *et al.* showed that p38 is critical for the IL-1 β -induced production of IL-6. IL-6 mRNA stability is promoted by p38 via interactions with the IL-6 3' UTR in

MEF cells. However, LPS had no effect on IL-6 expression (30), suggesting that the production of the IL-6 mRNA and its stability depend upon the cell type and the type of stimulus being applied to activate the p38 MAPK.

p38 MAPK has previously been shown to be involved in the phosphorylation-induced degradation of its substrates. For example, p38 MAPK phosphorylates p300, a co-transcriptional factor that is involved in chromatin remodeling, at Ser-1834, leading to the degradation of p300 during DNA damage responses (31,32). Our data showed that the phosphorylation of Arid5a at Ser-258, Ser-433 and Ser-458 is facilitated by p38 MAPK during the late phase of TLR4 stimulation and that this initiates the ubiquitin proteasome-dependent degradation of Arid5a. Disrupting these phosphorylation sites abrogated the p38-mediated degradation of the Arid5a protein. Interestingly, these phos-

phorylation sites are conserved among species as distantly related as humans and rats. Although Arid5a clearly interacted with IKK α and IKK β , these factors did not promote its phosphorylation. It would be interesting to determine the functional relevance of this protein interaction.

Chi *et al.* previously reported that the MAPKs play reciprocating roles in the temporal regulation of both pro- and anti-inflammatory cytokines (10). During the initial phase of macrophage activation, the rapid synthesis of pro-inflammatory cytokines is incompletely mediated by MAPKs, which may trigger an increase in the expression of MKP-1 (33,34). However, the upregulation of MKP-1 following stimulation is transitory, and when the suppressive effect of MKP-1 phosphatase activity is removed, p38 MAPK levels again increase over time (15). The initial induction of MKP-1 serves to restrain the excessive production of Arid5a and destabilize its mRNA via AUF-1, as discussed above. The subsequent substantial downregulation of MKP-1 that begins at 6 h or more after stimulation (data not shown) allows the remaining active p38 MAPK to induce the phosphorylation-mediated degradation of Arid5a. WWP1 E3 ubiquitin ligase was previously reported to induce the proteasomal degradation of TRAF6 via K48-linked polyubiquitination in response to LPS (35). Consistent with the previous study, our data suggest that WWP1 facilitates the degradation of Arid5a via K48-linked ubiquitination in TLR4 signaling.

We showed that an Arid5a phosphorylation-resistant mutant was associated with an overwhelming response to the expression of IL-6 mRNA. Moreover, this mutant Arid5a exhibited more potent functions than those of the WT Arid5a, possibly because of the prolonged existence of the mutant Arid5a during the late phase of LPS signaling, which resulted in the overproduction of IL-6 via its previously known IL-6 mRNA-stabilizing function.

In conclusion, we explored the signaling pathways underlying the regulation of Arid5a in response to TLR4 signaling and showed that Arid5a influences the half-life of IL-6 mRNA in cells stimulated with TLR4 (Supplementary Figure S5). Although Arid5a is initially rapidly upregulated, it is subsequently destabilized and degraded in response to TLR4. Moreover, the mechanisms underlying these two dynamic processes are mediated by IKK/NF- κ B and MAPK (through MKP-1/AUF-1 and p38 MAPK-mediated phosphorylation) signaling, respectively. Based on these key observations, we propose that these regulatory mechanisms accomplish both the suppression of unwanted inflammation and the production of pro-inflammatory cytokines, especially IL-6, in response to infection with pathogens.

SUPPLEMENTARY DATA

Supplementary Data are available at NAR Online.

ACKNOWLEDGEMENTS

K.K.N. acknowledges JSPS for postdoctoral fellowships for overseas researchers. We thank Prof. S. Akira and Dr T. Satoh (Osaka University) for the pCMV-AUF-1 expression plasmid, Prof. M. Yamamoto (Osaka University) for the hemagglutinin-tagged ubiquitin and Flag-tagged STAT3,

Prof. K. Yoshioka (Kanazawa University) for the Flag-tagged JNK-1 and JNK-2; Addgene for p65 and c-Rel; and Prof. T. Okamoto for preparing the viruses during the immortalization of primary MEF cells.

FUNDING

Japan Society for the Promotion of Science (JSPS) KAKENHI Grants-in-Aid [25.03097, 15F15907]; Kishimoto Foundation; JSPS Postdoctoral Fellowships [P13097, PU15907 to K.K.N.]. Funding for open access charge: Kishimoto Foundation; JSPS [15F15907].

Conflict of interest statement. None declared.

REFERENCES

- Kawai,T. and Akira,S. (2011) Toll-like receptors and their crosstalk with other innate receptors in infection and immunity. *Immunity*, **34**, 637–650.
- Medzhitov,R. and Horng,T. (2009) Transcriptional control of the inflammatory response. *Nat. Rev. Immunol.*, **9**, 692–703.
- Kishimoto,T. (2005) INTERLEUKIN-6: from basic science to medicine—40 years in immunology. *Annu. Rev. Immunol.*, **23**, 1–21.
- Anderson,P. (2008) Post-transcriptional control of cytokine production. *Nat. Immunol.*, **9**, 353–359.
- Hao,S. and Baltimore,D. (2009) The stability of mRNA influences the temporal order of the induction of genes encoding inflammatory molecules. *Nat. Immunol.*, **10**, 281–288.
- Matsushita,K., Takeuchi,O., Standley,D.M., Kumagai,Y., Kawagoe,T., Miyake,T., Satoh,T., Kato,H., Tsujimura,T., Nakamura,H. *et al.* (2009) Zc3h12a is an RNase essential for controlling immune responses by regulating mRNA decay. *Nature*, **458**, 1185–1190.
- Masuda,K., Ripley,B., Nishimura,R., Mino,T., Takeuchi,O., Shioi,G., Kiyonari,H. and Kishimoto,T. (2013) Arid5a controls IL-6 mRNA stability, which contributes to elevation of IL-6 level in vivo. *Proc. Natl. Acad. Sci. U.S.A.*, **110**, 9409–9414.
- Iwasaki,H., Takeuchi,O., Teraguchi,S., Matsushita,K., Uehata,T., Kuniyoshi,K., Satoh,T., Saitoh,T., Matsushita,M., Standley,D.M. *et al.* (2011) The I κ B kinase complex regulates the stability of cytokine-encoding mRNA induced by TLR–IL-1R by controlling degradation of regnase-1. *Nat. Immunol.*, **12**, 1167–1175.
- Schoenberg,D.R. and Maquat,L.E. (2012) Regulation of cytoplasmic mRNA decay. *Nat. Rev. Genet.*, **13**, 246–259.
- Chi,H., Barry,S.P., Roth,R.J., Wu,J.J., Jones,E.A., Bennett,A.M. and Flavell,R.A. (2006) Dynamic regulation of pro- and anti-inflammatory cytokines by MAPK phosphatase 1 (MKP-1) in innate immune responses. *Proc. Natl. Acad. Sci. U.S.A.*, **103**, 2274–2279.
- Yu,H., Sun,Y., Haycraft,C., Palanisamy,V. and Kirkwood,K.L. (2011) MKP-1 regulates cytokine mRNA stability through selectively modulation subcellular translocation of AUF1. *Cytokine*, **56**, 245–255.
- Keyse,S.M. (2000) Protein phosphatases and the regulation of mitogen-activated protein kinase signalling. *Curr. Opin. Cell Biol.*, **12**, 186–192.
- Liu,Y., Shepherd,E.G. and Nelin,L.D. (2007) MAPK phosphatases — regulating the immune response. *Nat. Rev. Immunol.*, **7**, 202–212.
- Manetsch,M., Che,W., Seidel,P., Chen,Y. and Ammit,A.J. (2012) MKP-1: a negative feedback effector that represses MAPK-mediated pro-inflammatory signaling pathways and cytokine secretion in human airway smooth muscle cells. *Cell. Signal.*, **24**, 907–913.
- Prabhala,P., Bunge,K., Rahman,M.M., Ge,Q., Clark,A.R. and Ammit,A.J. (2015) Temporal regulation of cytokine mRNA expression by tristetraprolin: dynamic control by p38 MAPK and MKP-1. *Am. J. Physiol. Lung Cell. Mol. Physiol.*, **308**, L973–L980.
- Mahtani,K.R., Brook,M., Dean,J.L.E., Sully,G., Saklatvala,J. and Clark,A.R. (2001) Mitogen-activated protein kinase p38 controls the expression and posttranslational modification of tristetraprolin, a regulator of tumor necrosis factor alpha mRNA stability. *Mol. Cell. Biol.*, **21**, 6461–6469.

17. Lafarga, V., Cuadrado, A., de Silanes, I., Bengoechea, R., Fernandez-Capetillo, O. and Nebreda, A.R. (2009) p38 mitogen-activated protein kinase- and HuR-dependent stabilization of p21Cip1 mRNA mediates the G1/S checkpoint. *Mol. Cell. Biol.*, **29**, 4341–4351.
18. Kirkwood, K. and Rossa, J.C. (2009) The potential of p38 MAPK inhibitors to modulate periodontal infections. *Curr. Drug Metab.*, **10**, 55–67.
19. Amano, K., Hata, K., Muramatsu, S., Wakabayashi, M., Takigawa, Y., Ono, K., Nakanishi, M., Takashima, R., Kogo, M., Matsuda, A. *et al.* (2011) Arid5a cooperates with Sox9 to stimulate chondrocyte-specific transcription. *Mol. Biol. Cell.*, **22**, 1300–1311.
20. Masuda, K., Ripley, B., Nyati, K.K., Dubey, P.K., Zaman, M.M.-U., Hanieh, H., Higa, M., Yamashita, K., Standley, D.M., Mashima, T. *et al.* (2016) Arid5a regulates naive CD4 + T cell fate through selective stabilization of Stat3 mRNA. *J. Exp. Med.*, **213**, 605–619.
21. Limbach, H.J., Arnold, A., Mann, B.A. and Holm, C. (2006) ESPResSo—an extensible simulation package for research on soft matter systems. *Comput. Phys. Commun.*, **174**, 704–727.
22. Li, S., Yamashita, K., Amada, K.M. and Standley, D.M. (2014) Quantifying sequence and structural features of protein-RNA interactions. *Nucleic Acids Res.*, **42**, 10086–10098.
23. Chen, L.F., Williams, S.A., Mu, Y., Nakano, H., Duerr, J.M., Buckbinder, L. and Greene, W.C. (2005) NF- κ B RelA phosphorylation regulates RelA acetylation. *Mol. Cell. Biol.*, **25**, 7966–7975.
24. Jackson, R.J. (1993) Cytoplasmic regulation of mRNA function: the importance of the 3' untranslated region. *Cell*, **74**, 9–14.
25. Paschoud, S., Dogar, A.M., Kuntz, C., Grisoni-Neupert, B., Richman, L. and Kuhn, L.C. (2006) Destabilization of interleukin-6 mRNA requires a putative RNA stem-loop structure, an AU-rich element, and the RNA-binding protein AUF1. *Mol. Cell. Biol.*, **26**, 8228–8241.
26. Ghosh, S., May, M.J. and Kopp, E.B. (1998) NF-kappa B and Rel proteins: evolutionarily conserved mediators of immune responses. *Annu. Rev. Immunol.*, **16**, 225–260.
27. Grivennikov, S. and Karin, M. (2008) Autocrine IL-6 signaling: a key event in tumorigenesis? *Cancer Cell*, **13**, 7–9.
28. Saito, Y., Kagami, S.-I., Sanayama, Y., Ikeda, K., Suto, A., Kashiwakuma, D., Furuta, S., Iwamoto, I., Nonaka, K., Ohara, O. *et al.* (2014) AT-rich-interactive domain-containing protein 5A functions as a negative regulator of retinoic acid receptor-related orphan nuclear receptor γ t-induced Th17 cell differentiation. *Arthritis Rheumatol.*, **66**, 1185–1194.
29. Zhao, W., Liu, M., D'Silva, N.J. and Kirkwood, K.L. (2011) Tristetraprolin regulates interleukin-6 expression through p38 MAPK-dependent affinity changes with mRNA 3' untranslated region. *J. Interferon Cytokine Res.*, **31**, 629–637.
30. Zhao, W., Liu, M. and Kirkwood, K.L. (2008) p38 α stabilizes interleukin-6 mRNA via multiple AU-rich elements. *J. Biol. Chem.*, **283**, 1778–1785.
31. Poizat, C., Puri, P.L., Bai, Y. and Kedes, L. (2005) Phosphorylation-dependent degradation of p300 by doxorubicin-activated p38 mitogen-activated protein kinase in cardiac cells. *Mol. Cell. Biol.*, **25**, 2673–2687.
32. Wang, Q.E., Han, C., Zhao, R., Wani, G., Zhu, Q., Gong, L., Battu, A., Racoma, I., Sharma, N. and Wani, A.A. (2013) p38 MAPK- and Akt-mediated p300 phosphorylation regulates its degradation to facilitate nucleotide excision repair. *Nucleic Acids Res.*, **41**, 1722–1733.
33. Dong, C., Davis, R.J. and Flavell, R.A. (2002) MAP kinases in the immune response. *Annu. Rev. Immunol.*, **20**, 55–72.
34. de waal Malefyt, R., Abrams, J., Bennett, B., Figdor, C.G. and de Vries, J.E. (1991) Interleukin 10 (IL-10) inhibits cytokine synthesis by human monocytes: an autoregulatory role of IL-10 produced by monocytes. *J. Exp. Med.*, **174**, 1209–1220.
35. Lin, X.-W., Xu, W.-C., Luo, J.-G., Guo, X.-J., Sun, T., Zhao, X.-L. and Fu, Zhi-Jian. (2013) WW domain containing E3 ubiquitin protein ligase 1 (WWP1) negatively regulates TLR4-mediated TNF- α and IL-6 production by proteasomal degradation of TNF receptor associated factor 6 (TRAF6). *PLoS One.*, **8**, e67633.